ilmedia

Technische Universität ILMENAU

Xu, Changfan; Dong, Yulian; Shen, Yonglong; Zhao, Huaping; Li, Liqiang; Shao, Guosheng; Lei, Yong

Fundamental understanding of nonaqueous and hybrid Na-CO2 batteries: challenges and perspectives

Fundamental Understanding of Nonaqueous and Hybrid Na–CO₂ Batteries: Challenges and Perspectives

Changfan Xu, Yulian Dong, Yonglong Shen, Huaping Zhao, Liqiang Li, Guosheng Shao,* and Yong Lei*

Alkali metal–CO₂ batteries, which combine CO₂ recycling with energy conversion and storage, are a promising way to address the energy crisis and global warming. Unfortunately, the limited cycle life, poor reversibility, and low energy efficiency of these batteries have hindered their commercialization. Li–CO₂ battery systems have been intensively researched in these aspects over the past few years, however, the exploration of Na–CO₂ batteries is still in its infancy. To improve the development of Na–CO₂ batteries, one must have a full picture of the chemistry and electrochemistry controlling the operation of Na–CO₂ batteries and a full understanding of the correlation between cell configurations and functionality therein. Here, recent advances in CO₂ chemical and electrochemical mechanisms on nonaqueous Na–CO₂ batteries and hybrid Na–CO₂ batteries (including O₂-involved Na–O₂/CO₂ batteries) are reviewed in-depth and comprehensively. Following this, the primary issues and challenges in various battery components are identified, and the design strategies for the interfacial structure of Na anodes, electrolyte properties, and cathode materials are explored, along with the correlations between cell configurations, functional materials, and comprehensive performances are established. Finally, the prospects and directions for rationally constructing Na–CO₂ battery materials are foreseen.

C. Xu, Y. Dong, H. Zhao, Y. Lei
Fachgebiet Angewandte Nanophysik
Institut für Physik & IMN MacroNano
Technische Universität Ilmenau
98693 Ilmenau, Germany
E-mail: yong.lei@tu-ilmenau.de
Y. Shen, G. Shao
School of Materials Science and Engineering
Zhengzhou University
Zhengzhou 450001, China
E-mail: gsshao@zzu.edu.cn
L. Li
Tianjin Key Laboratory of Molecular Optoelectronic Sciences
Department of Chemistry
Institute of Molecular Aggregation Science
Tianjin University
Tianjin 300072, China

The ORCID identification number(s) for the author(s) of this article can be found under https://doi.org/10.1002/smll.202206445.

1. Introduction

Rapid economic and social development has brought humanity a rich material civilization, but also intensified the large-scale consumption of fossil fuel energy.[1,2] The accompanying energy crisis, environmental pollution, and global warming caused by rapid carbon dioxide (CO₂) emissions have become serious problems that limit the sustainable development of humanity.[2,3] Following the "Paris Agreement" in 2015, more and more countries and regions have implemented the goal of net-zero greenhouse gas emissions into their development strategies, proposing a "zero-carbon" or "carbon neutral" climate goal.[4,5] The construction of a clean, low-carbon, secure, and efficient new energy system has emerged as the key to achieving this goal. As new energy power generation and grid energy storage have been rapidly developed, more demands are being placed on electrochemical power sources and energy storage systems. Lithium-ion batteries (LIBs), as one of the most amazing modern electrochemical energy storage technologies, are limited by low theoretical specific energy densities (usually lower than 700 Wh kg⁻¹) and even lack sufficient durability and affordability to fulfill practical demands.[6,7] Therefore, it is imperative to develop new secondary battery systems with higher energy densities to cope with future large-scale power storage and transportation power utilization.

Alkali metal–CO₂ batteries equipped with advanced CO₂ electrodes offer a promising strategy for the recycling and usage of CO₂ and electrochemical energy conversion and storage.[8,9] For example, Li–CO₂ and Na–CO₂ batteries offer theoretical specific energies as high as 1876 and 1125 Wh kg⁻¹, respectively (according to reactions of 4Li (Na) + 3CO₂ ↔ 2Li₂CO₃ (Na₂CO₃) + C), which are much higher than those of LIBs.[10,11] Regrettably, the research related to Na–CO₂ batteries is only the tip of the iceberg in comparison with the intensive exploration of Li–CO₂ batteries. In fact, the low free energy ($\Delta_r G^{\ominus} = -905.6$ kJ mol⁻¹) generated by the interaction involving Na and CO₂ results in a decreased charging potential than that of Li ($\Delta_r G^{\ominus} = -1081$ kJ mol⁻¹),[11] favoring the inhibition of electrolyte decomposition and contributes to a higher round-trip efficiency and extend lifetime, demonstrating great potential for

Na–CO2 batteries. Typically, two types of Na–CO2 batteries have been investigated so far, namely, nonaqueous and aqueous batteries. Nonaqueous systems are usually equipped with aprotic or solid-state electrolytes (defined as aprotic and solid-state Na–CO2 batteries), where products are mainly carbonates.[11,12] It may seem to be counterintuitive, but aqueous systems can be implemented with a protective membrane separating the sodium metal from the aqueous electrolytes (defined as hybrid Na–CO2 batteries).[13,14] The use of aqueous electrolytes in Na–CO2 batteries can solve problems associated with insoluble and insulating carbonate products in nonaqueous systems, and there is potential for CO2 conversion to a variety of value-added chemicals in hybrid Na–CO2 batteries according to the proton-coupled electron transfer mechanism.[13,15] Although Na–CO2 batteries are still in their infancy, there is no doubt about their inherent advantages in related to energy storage and CO2 utilization (**Figure 1**a): i) Storage of green electricity supplied by intermittent renewable energy sources, including solar, wind, and tidal energy, etc.; ii) conversion of CO2 into reusable and renewable chemicals, such as CO, CH4, methanol, formic acid, etc.; iii) electricity supply in daily life and industrial production, helping to build a low carbon economy and "zero-carbon" network; iv) alternative energy sources for space exploration and underwater operations, as well as, energy storage in CO2-rich environments, such as the Martian atmosphere.

Na–CO2 batteries with high specific energy density were derived from research on CO2-contaminated gas in Na–O2 batteries with the aim of achieving practical applications in the air.[16–19] It is known that the dissolution of CO2 in organic electrolytes is higher than that of O2 (about 50 times higher than O2), and CO2 in ambient air is extremely susceptible to participate in Na–O2 battery reaction to form Na2CO3. Na2CO3 is a broad bandgap insulator that requires a higher decomposition potential than NaO2 and Na2O2, tending to cause capacity deterioration, poor reversibility, and worse cycling.[20,21] CO2/O2 mixes or pure CO2 atmospheres must be evaluated for their effects on Na–O2 batteries. Thus, studies on Na–CO2 batteries were triggered by Archer and his co-workers in 2012.[16] They found that Na–O2/CO2 batteries with an optimized CO2 concentration displayed an increased discharge capacity of more than 2 folds compared to the Na–O2 batteries. More interestingly, the battery also showed a low discharge capacity in a pure CO2 atmosphere, demonstrating that CO2 itself can be exploited as a reaction gas. A breakthrough was achieved in 2016 when Hu et al. introduced the first rechargeable nonaqueous Na–CO2 battery that operated at room temperature in a nonaqueous organic electrolyte.[11] The rechargeable Na–CO2 battery achieved high discharge capacity and remained stable cycling over 200 cycles, which triggered the high research attention of Na–CO2 batteries. Afterward, the electrochemical performances of Na–CO2 batteries have been gradually improved by developing novel cathodes and efficient catalysts, as well as modifying the anode surface and regulating the electrolyte (Figure 1b).[22–32] Intriguingly, the first rechargeable hybrid Na–CO2 battery with an aqueous catholyte was reported in 2018, which can continuously generate electrical energy during discharge, while hydrogen was produced during charging, rather than CO2.[13] Conceptually, in CO2 aqueous electrolysis, water is considered to be a good medium to donate protons for CO2

electrochemistry with tunable products when assisted by specific electrocatalysts.[33] Accordingly, hybrid Na–CO2 batteries that utilize a proton-coupled electron transfer mechanism to boost flexible CO2 electrochemistry demonstrate great applications in clean energy storage, CO2 mitigation, and production of value-added chemicals.

Indisputably, both non-aqueous and aqueous Na–CO2 batteries have their advantages and disadvantages. Several daunting issues, including slow CO2 electrochemical kinetics, notoriously low reversibility and cycling stability, as well as, low round-trip efficiency, overshadow any practical application of Na–CO2 batteries.[34–36] Therefore, extensive research must be conducted before they can be commercially exploited. A fundamental understanding of Na–CO2 electrochemistry, developing new and modified battery materials, and innovating on key components of battery design are requested. In the past, several groups have reviewed the research efforts on metal–CO2 batteries, mainly Li–CO2 batteries.[8,9,37–39] Specifically, Zhou et al.[40] published a valuable review in 2020 that discussed the impact of reaction conditions on the mechanism of Li–CO2 and Na–CO2 batteries. It is important to highlight that the mechanism of Na–CO2 electrochemistry, particularly for hybrid Na–CO2 batteries, was unclear at the early stage, and there were limited reports on Na anode protection, electrolyte, and cathode materials. Much progress has been made in the last 2 years in research on the reaction mechanisms and functional materials of Na–CO2 batteries, but a thorough and understandable analysis of the relationship between Na–CO2 battery components and their functionality is not available. In particular, the specific focus on hybrid Na–CO2 batteries lacks summarizations. Herein, a comprehensive report is presented that covers the reaction mechanisms, challenges, potential solutions, and recent advancements related to Na–CO2 batteries. We anticipate that this review will provide readers with a clear picture of what Na–CO2 and associated batteries stand to gain going forward.

2. Diversity and Electrochemical Mechanisms

2.1. Configuration of Na–CO2 Batteries

Typically, Na–CO2 batteries consist of sodium metal as the negative electrode (i.e., the anode) and CO2 diffusion cathode (CO2 as the cathode reactant) at the current stage, where the CO2 cathode commonly is a highly porous electrode that enables electrochemical contact between CO2 and sodium ions. Its main function is to dissolve/deposit sodium metal at the anode and to carry out the electrochemical conversion of CO2 at the cathode. The illustrations of aprotic, solid-state, and hybrid Na–CO2 batteries and their corresponding performances are presented in **Figure 2**. The radar plot qualitatively describes the main pros and cons of the three Na–CO2 batteries based on six important metrics for electrochemical energy storage devices.[46–49] What distinguishes them is the type of electrolyte involved, which affects the exact electrochemical reactions and properties that occur during CO2 recycling applications and energy storage.

In the aprotic Na–CO2 battery (Figure 2a), two electrodes are separated by a Na+ conducting membrane (e.g., glass fiber
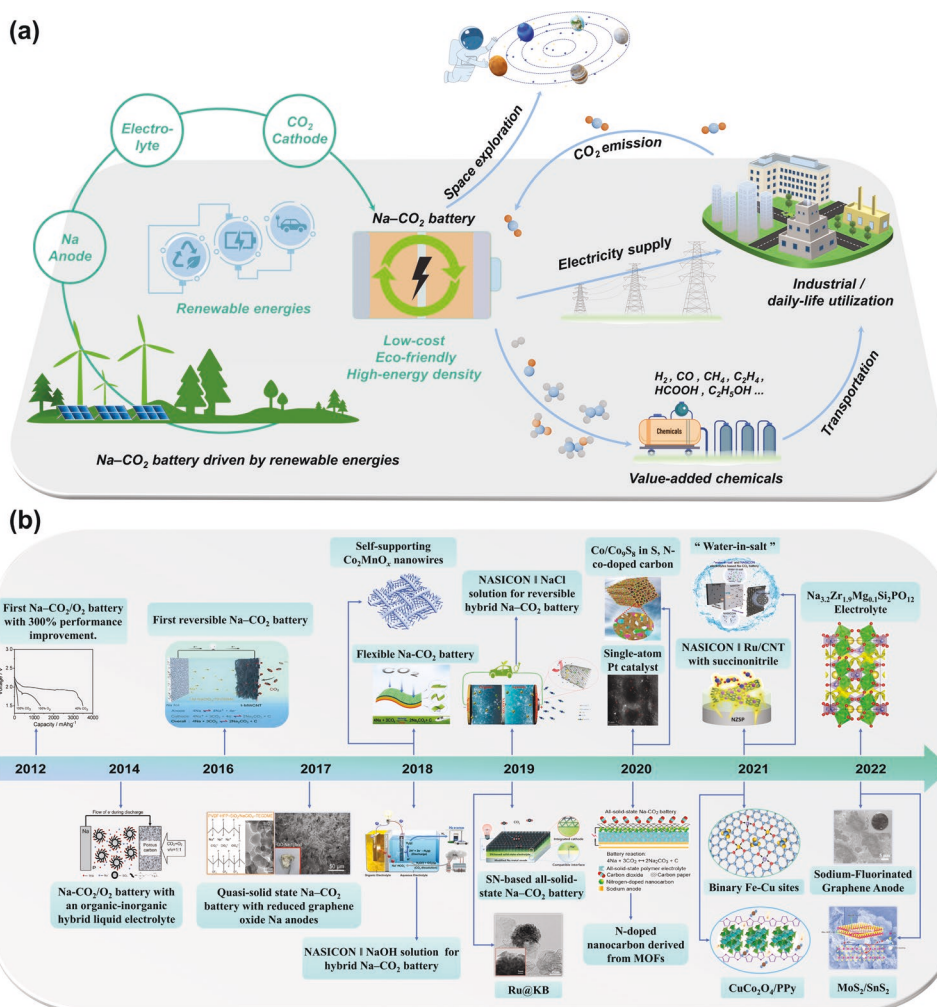
Figure 1. a) Schematic diagram of a Na–CO$_2$ battery system driven by renewable energy. A "zero-carbon" network is achieved by storing renewable energy and reducing CO$_2$ in Na–CO$_2$ batteries to generate electricity and valuable products that can be reused and recycled. b) A brief timeline of the scientific progress on Na–CO$_2$ batteries, including representative sodium metal protection, cathode design, and electrolyte optimization. Inset images: first Na–CO$_2$/O$_2$ battery with 300% performance improvement. Reproduced with permission.[16] Copyright 2013, Elsevier. Na–CO$_2$/O$_2$ battery with an organic–inorganic hybrid liquid electrolyte. Reproduced with permission.[41] Copyright 2014, Royal Society of Chemistry. First reversible Na–CO$_2$ battery. Reproduced with permission.[11] Copyright 2016, Wiley-VCH. Quasi-solid state Na–CO$_2$ battery with reduced graphene oxide Na anodes. Reproduced with permission.[30] Copyright 2017, American Association for the Advancement of Science. NASICON ∥ NaOH solution for hybrid Na–CO$_2$ battery. Reproduced with permission.[13] Copyright 2018, Elsevier. Flexible Na–CO$_2$ battery. Reproduced with permission.[12] Copyright 2018, Wiley-VCH. Self-supporting Co$_2$MnO$_x$ nanowires. Reproduced with permission.[26] Copyright 2018, American Chemical Society. NASICON ∥ NaCl solution for reversible hybrid Na–CO$_2$ battery. Reproduced with permission.[14] Copyright 2020, Elsevier. SN-based all-solid-state Na–CO$_2$ battery. Reproduced with permission.[24] Copyright 2019, Royal Society of Chemistry. Ru@KB. Reproduced with permission.[22] Copyright 2019, Royal Society of Chemistry. N-doped nanocarbon derived from MOFs. Reproduced with permission.[25] Copyright 2020, American Chemical Society. Single-atom Pt catalyst. Reproduced with permission.[29] Copyright 2020, Elsevier. Co/Co$_9$S$_8$ in S, N-co-doped carbon. Reproduced with permission.[42] Copyright 2020, Elsevier. "Water-in-salt." Reproduced with permission.[31] Copyright 2021, Elsevier. NASICON ∥ Ru/CNT with succinonitrile. Reproduced with permission.[32] Copyright 2021, Elsevier. Binary Fe-Cu sites. Reproduced with permission.[43] Copyright 2021, Royal Society of Chemistry. CuCo$_2$O$_4$/PPy. Reproduced with permission.[44] Copyright 2021, Elsevier. Na$_{3.2}$Zr$_{1.9}$Mg$_{0.1}$Si$_2$PO$_{12}$ electrolyte. Reproduced with permission.[27] Copyright 2022, Wiley-VCH. MoS$_2$/SnS$_2$. Reproduced with permission.[28] Copyright 2022, American Chemical Society. Sodium-fluorinated graphene anode. Reproduced with permission.[45] Copyright 2021, Wiley-VCH.

separator) immersed in an organic electrolyte that is made of a sodium salt dissolved in a nonaqueous organic solvent. During the discharge process, sodium metal is oxidized at the anode, forming sodium ions and electrons, which travel to the CO$_2$ cathode by means of the electrolyte and external circuit, respectively; whereas CO$_2$ is reduced at the catalytic CO$_2$ electrode surface and forms the solid discharge product, presumably Na$_2$CO$_3$.[11] When the battery is charged, involving the decomposition of solid Na$_2$CO$_3$ in the cathode and sodium metal plating at the anode.[50] The utilization of catalytic porous CO$_2$ electrodes is consequently crucial for an aprotic Na–CO$_2$ battery, which not only contributes to the storage of insoluble discharge products but also facilitates the CO$_2$ reduction reaction (CRR, Na$_2$CO$_3$ formation) and CO$_2$ evolution reactions (CER,

ADVANCED
SCIENCE NEWS
www.advancedsciencenews.com
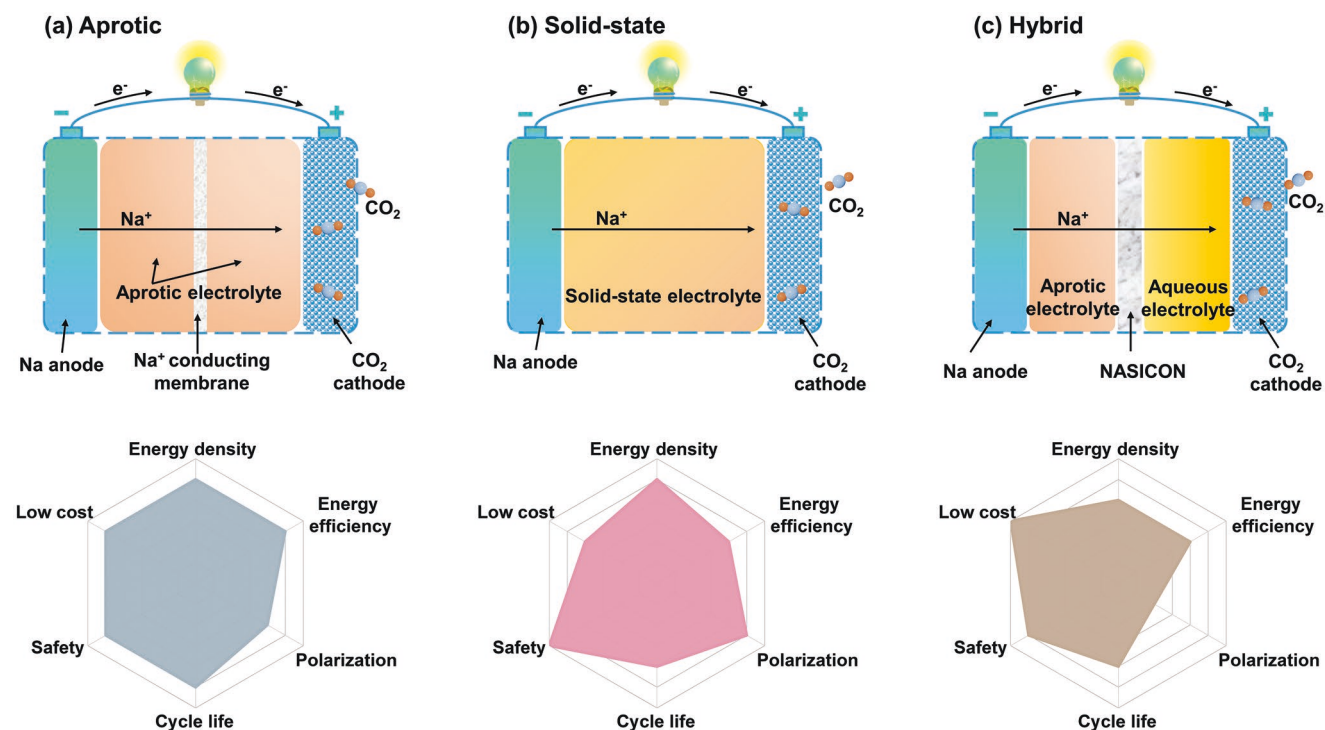
NANO · MICRO
small
www.small-journal.com

Figure 2. Schematic illustration and the corresponding performances of a) aprotic Na–CO$_2$ battery, b) all-solid-state Na–CO$_2$ battery, and c) hybrid Na–CO$_2$ battery.

Na$_2$CO$_3$ decomposition) during the discharging and charging of batteries.[42]

Solid-state Na–CO$_2$ batteries (Figure 1b) without involving any liquid electrolytes have also been developed to eliminate the problems of leakage, drying, and refilling of the liquid electrolyte. To date, two main solid-state sodium ion conducting materials are already employed in Na–CO$_2$ batteries, one being a polymer electrolyte and the other being a NASICON-type (Na superionic conductor) inorganic solid ceramic electrolyte.[12,32] Polymer solid-state electrolytes with soft and flexible textures allowing them to be in close contact with the electrodes are widely used to build up solid-state Na–CO$_2$ batteries, which will also benefit the application of future wearable electronic devices.[12,51] Inorganic solid electrolytes have intrinsic characteristics such as non-flammability, wide electrochemical window, good thermal stability, and non-toxicity, but their application is restricted owing to the poor compatibility and stability of the sodium metal anode/inorganic solid electrolyte/CO$_2$ cathode interface.[52] The fundamental mechanism of the solid-state system may be similar to that of the aprotic system, unfortunately, the excessive accumulation of Na$_2$CO$_3$ on the solid-state electrolyte and CO$_2$ cathode interface in the solid-state system severely contributes to premature battery failure.[12,25] Genuinely, solid-state Na–CO$_2$ batteries are not only challenged by the limited availability of solid-state conducting materials with sufficient sodium ion conductivity, but also by how much Na$_2$CO$_3$ can be deposited in the CO$_2$ cathode.

The performances of two nonaqueous batteries are mainly limited by blockage of solid insoluble discharge products and passivation of the active surfaces of the CO$_2$ cathode. Hybrid Na–CO$_2$ batteries with aqueous catholyte have been proposed as an effective strategy for dealing with the problem of solid insoluble Na$_2$CO$_3$ in nonaqueous batteries.[14] Normally, the hybrid Na–CO$_2$ battery (Figure 2c) uses both organic and aqueous electrolytes, the anode compartment is designed similarly to that of an aprotic Na–CO$_2$ battery, whereas the CO$_2$ cathode electrode is immersed in the aqueous catholyte.[13,14] A protective layer for Na metal and organic anolyte is necessary to enable the desired electrochemistry, which not only separates the organic anolyte and aqueous catholyte physically but also eliminates possible contamination of Na metal and the organic anolyte by H$_2$O and CO$_2$, as well as avoids internal short-circuit interaction between the Na dendrite and the CO$_2$ cathode.[47,48] NASICON solid ceramic electrolyte as a protective layer allowing only Na$^+$ ions to be transported has been deeply studied in the hybrid system.[14,31] Notably, the chemistry of hybrid Na–CO$_2$ batteries is slightly different from that of nonaqueous systems, which depend on the aqueous catholyte and CO$_2$ cathode. For instance, the hybrid batteries detected NaHCO$_3$ as the main discharge product when using saturated NaCl solution as the catholyte and carbon materials as the cathode.[14,42,43] In contrast, the hybrid Na–CO$_2$ battery used NaOH solution as the catholyte and a composite of Pt/C and IrO$_2$ as the catalytic cathode to produce hydrogen during discharge.[13] Although H$_2$O as a solvent does lead to an increase in sodium ion conductivity and enhanced electrochemical reaction kinetics, the specific energy of hybrid batteries is lower than that of nonaqueous Na–CO$_2$ batteries when taking into account the overall reactants because of the different electrochemical reactions involving metals and CO$_2$.[15,33]

ADVANCED
SCIENCE NEWS
www.advancedsciencenews.com

NANO · MICRO
small
www.small-journal.com

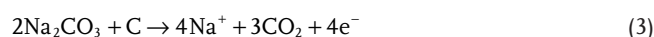## 2.2. Discharge–Charge Mechanisms of Nonaqueous Na–CO$_2$ Batteries

2.2.1. Reactions Involving Oxygen

In 2012, the Archer's group first presented primary non-aqueous Na–O$_2$/CO$_2$ batteries for capturing CO$_2$ and generating electricity.[16] The Na–O$_2$/CO$_2$ batteries were operational at room temperature and used Super P carbon as the cathode, sodium metal as the anode, and an electrolyte made up of either NaClO$_4$ in tetraethylene glycol dimethyl ether (TEGDME) or NaCF$_3$SO$_3$ in 1-ethyl-3-methylimidazolium trifluoromethane-sulfonate (IL). X-ray diffraction (XRD) and Fourier transform infrared spectroscopy analysis indicated that both Na$_2$CO$_3$ and Na$_2$C$_2$O$_4$ coexisted in TEGDME-based battery, whereas Na$_2$C$_2$O$_4$ was the main product in the IL-based battery. Na$_2$O$_2$ was not discovered in the Na–CO$_2$/O$_2$ batteries. They, therefore, proposed possible discharge mechanisms, as shown in **Figure 3**a. Mechanism 1 involves first the one-electron reduction of O$_2$, forming the superoxide radicals (O$_2^{\bullet-}$). As a powerful nucleophile, the generated O$_2^{\bullet-}$ can create oxalate radical anion (CO$_4^{\bullet-}$) by bonding with the carbonyl carbon atoms of CO$_2$ molecules, and Na$_2$CO$_3$ is eventually generated via nucleophilic addition and reduction reactions with peroxodicarbonate anion (C$_2$O$_6^{2-}$) and CO$_4^{\bullet-}$ as intermediate. Mechanism 2 starts with a two-electron reduction of O$_2$ to form O$_2^{\bullet-}$, followed by a reaction with CO$_2$ to form CO$_4^{2-}$, which combines with sodium ions and CO$_2$ to form Na$_2$C$_2$O$_4$ and release O$_2$. Compared with O$_2$-involved electrochemical reduction in mechanisms 1 and 2, the reaction process of Mechanism 3 appears to be relatively simple. Upon capturing electrons from the cathode, dissolved CO$_2$ molecules can be further reduced to C$_2$O$_4^{2-}$ by one-electron reduction or to CO and produce Na$_2$CO$_3$ by two-electron reduction. Briefly, according to their hypothesis, the electrochemical processes followed first in mechanisms 1 and 2 are the "oxygen reduction reactions" in Na–O$_2$ electrochemistry, and subsequently the basic electrochemical/chemical reaction pathways involving the reduction of CO$_2$. The reactions in mechanism 3 do not involve O$_2$, which are purely electrochemical reductions of CO$_2$ in Na–CO$_2$ electrochemistry. Mechanisms 1 and 2 could exist simultaneously in Na–O$_2$/CO$_2$ batteries using the TEGDME-based electrolyte, while mechanism 2 was dominant in the IL-based electrolyte. Regrettably, the above reaction mechanisms were all hypothesized because of the inability to identify intermediates directly, so more convincing experiments are requested to verify their reliability.

Afterward, a rechargeable Na–O$_2$/CO$_2$ battery was proposed, which used a porous carbon cathode and an organic–inorganic hybrid electrolyte comprised of 1 M NaTFSI in propylene carbonate (PC) containing SiO$_2$ and ionic liquid (SiO$_2$-IL-TFSI/PC-NaTFSI).[41] Fascinatingly, NaHCO$_3$ was identified as the dominant discharge product in this work. An electrostatic intermittent titration technique (GITT) was also used to validate the equilibrium potential and conceivable reaction mechanisms were postulated, as shown in Figure 3b. The overall discharge potential of the reaction involving H$_2$ gas approaches the equilibrium value more closely than the reaction in which Na$_2$CO$_3$ is the main discharge product. It was speculated that the origin of H$_2$ gas was caused by the decomposition of the electrolyte

resulting in the formation of solid electrolyte interface (SEI). In addition, *ex situ* differential electrochemical mass spectrometry (DEMS) measurements with isotopic carbon were performed to track the evolution of gaseous products during charging. The evolution of CO$_2$ with both ^{13}C and ^{12}C had been observed, suggesting the decomposition of NaHCO$_3$ and the degradation of super P carbon cathode. However, no O$_2$ evolution was detected (Figure 3c), which was attributed to the parasitic reaction between evolved O$_2$ and carbon cathode. Also, no evolution of H$_2$ was detected either (Figure 3d), implying that the charging mechanism remains unknown. Not only that, but the discharge and charging mechanisms of Na–O$_2$/CO$_2$ batteries remain puzzling, as the discharge product Na$_2$CO$_3$ may be converted to NaHCO$_3$ in the presence of moisture and excess CO$_2$. Furthermore, the decomposition of the electrolyte and carbon-based cathode was undesirable during battery operation, contributing to a poor cycling performance of only 20 cycles. Then, the evolution of O$_2$ and CO$_2$ was detected when the carbon-based cathode was replaced with a strong nickel foam, with no significant side reactions, and cycle performance was improved to over 100 cycles.[53] All the above results indicate that the ratio of O$_2$ to CO$_2$, cathode materials, and properties of electrolytes have a significant impact on the performances, products, and reaction paths of Na–O$_2$/CO$_2$ electrochemistry; thus more adequate experimental evidence is needed to verify these proposed mechanisms.

Recently, Liu et al. reported an in situ study on the role of O$_2$ and CO$_2$ in Na–O$_2$/CO$_2$ batteries, revealing the structure and morphology of products during the charging and discharging process in real-time by employing an aberration-corrected environmental transmission electron microscope (AC ETEM).[54] They observed some core-shell spherical products growing on the carbon nanotubes (CNTs) during discharge, and these spherical products shrink until they disappear during charging (Figure 3e). In addition, CNTs became thinner at the end in contact with the sodium substrate during charging, which indicated that the CNTs could be consumed during the charging process. Characterization by electron diffraction pattern and electron energy loss spectroscopy (EELS) further demonstrated that the spherical products initially consisted of Na and Na$_2$O$_2$ and traces of Na$_2$CO$_3$, which were mostly chemically converted to Na$_2$CO$_3$ upon charging, and that Na$_2$CO$_3$ might eventually breakdown to generate Na and CO$_2$ with continued charging. The generation and degradation of Na$_2$CO$_3$ were reversible during repeated discharging and charging processes. The reaction mechanism was hence deduced to account for Na–O$_2$/CO$_2$ with CNTs as the cathode. During discharging, the Na$^+$ and the electrons meet O$_2$ to form Na$_2$O$_2$ through the discharge reaction of Equation (1); subsequently, Na$_2$O$_2$ undergoes a chemical reaction in a CO$_2$ atmosphere to become Na$_2$CO$_3$ (Equation (2)); During charging, CNTs are consumed to generate Na and CO$_2$ with Na$_2$CO$_3$, written as Equation (3).

$$2Na^+ + 2e^- + O_2 \rightarrow Na_2O_2 \tag{1}$$

$$Na_2O_2 + CO_2 \rightarrow Na_2CO_3 + O_2 \tag{2}$$

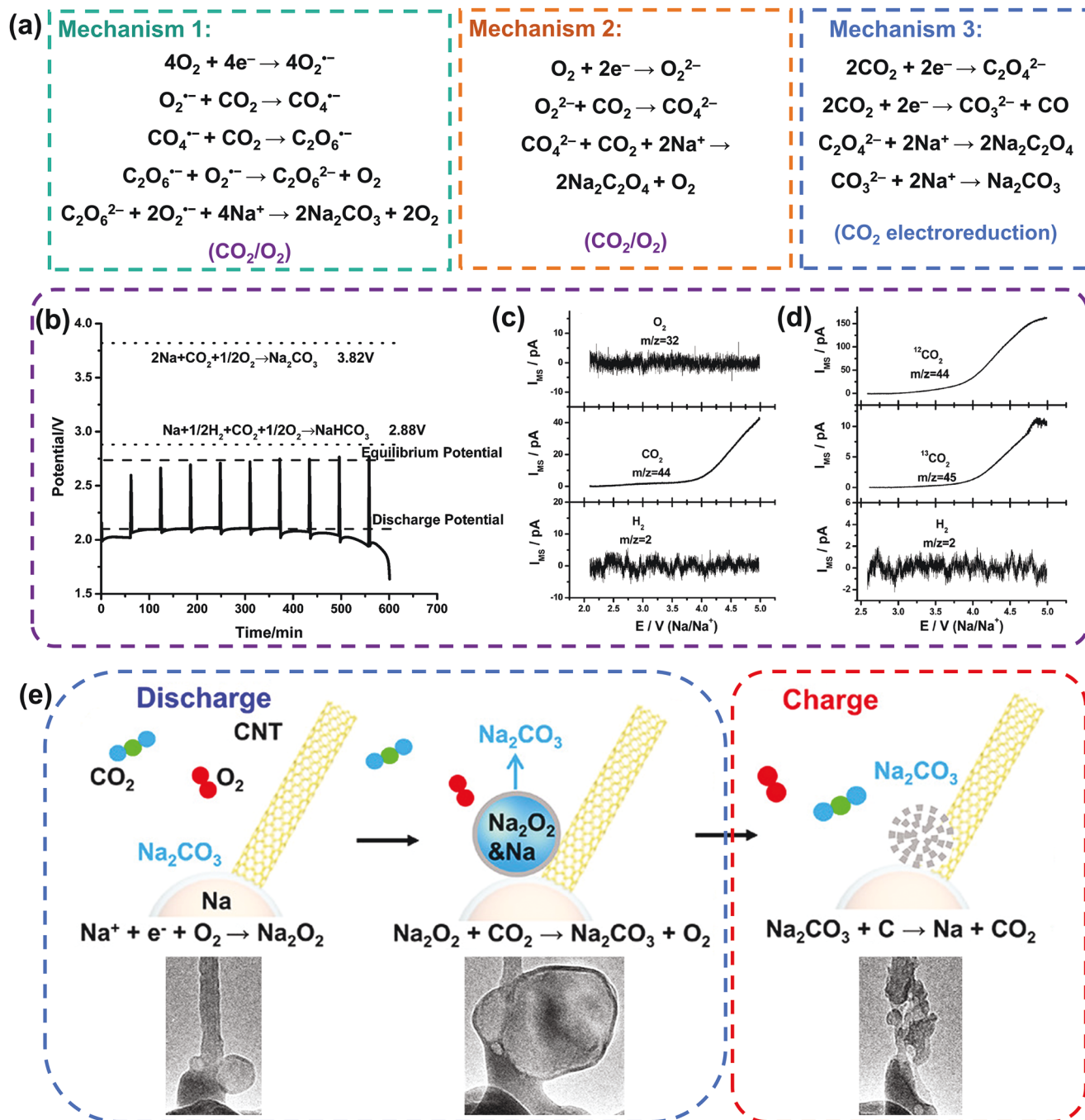$$2Na_2CO_3 + C \rightarrow 4Na^+ + 3CO_2 + 4e^- \tag{3}$$

Figure 3. a) The possible reaction mechanisms for Na-O₂/CO₂ electrochemistry. Reproduced with permission.[16] Copyright 2013, Elsevier. b) GITT discharge profile of Na-O₂/CO₂ cell with PC electrolyte with the dotted lines indicating the theoretical potentials; DEMS measurements of the Na-O₂/CO₂ battery with different cathodes: c) carbon black (super-P) cathode. d) Porous ¹³C cathode. b–d) Reproduced with permission.[41] Copyright 2014, Royal Society of Chemistry. e) Schematic representation of the discharge/charge reaction in the Na–CO₂/O₂ nanobattery. During discharge, the spherical structure of Na₂O₂ has been formed before the formation of Na₂CO₃ coating. The sphere shrinks during charging, generating Na and CO₂. Reproduced with permission.[54] Copyright 2020, American Chemical Society.

In the absence of CNTs, the discharge mechanism of the Na–O₂/CO₂ battery with Ag nanowires as cathodes showed the same reaction as that of the battery with CNTs as cathodes, the electrochemical decomposition of the Na_2CO_3 during charging could be described as Equation (4); however, the Na–O₂/CO₂ battery with Ag exhibited a very sluggish charging reaction and poor reversibility, implying that direct breakdown of Na_2CO_3 is challenging.

$$2Na_2CO_3 \rightarrow 4Na^+ + 2CO_2 + O_2 + 4e^- \qquad (4)$$
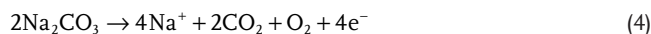
Without CO_2, the discharge process of the Na–O_2 battery took place via Equation (1), and the battery also showed poor cyclability because of the slow decomposition of Na_2O_2 during charging. Overall, carbon and CO_2 facilitate the electrochemical reaction process and improve the cycling capacity of the Na–O_2/CO_2 batteries. In addition, they also noticed that following discharge, a coating layer formed on the CNT that grew in thickness with the number of cycles and could not be removed, indicating the buildup of indecomposable discharge products or parasitic reaction products. The collection of undecomposable products on the cathode has been identified as a principal reason why metal–air batteries fail to operate in real air.[55,56] Their findings contribute to a better knowledge of electrochemistry underlying Na–O_2/CO_2 and Na–CO_2 batteries, which may assist in the future design of these battery systems.

What is clear is that in the above O_2-involved Na–CO_2 batteries, CO_2 is not involved in the electrochemical process, O_2 is the only electroactive substance and is mainly reduced. Regardless of the electrolyte, all of these Na–O_2/CO_2 batteries can provide an increased discharge capacity.[16] However, changing the electrolytes can alter the chemical route and the ultimate result. Similar phenomena have also been found in the Li–O_2/CO_2 electrochemical system,[10,57,58] and a more detailed discussion can be found in the excellent previous reviews on this topic by Zhou et al.[8,40] It was suggested the detailed reaction mechanisms of metal–O_2/CO_2 batteries were dependent on the reactivity between CO_2/metal ions and $O_2^{\bullet-}$, which were closely related to the nature of the electrolytes and, in particular, the donor number of solvents.[58,59] Notably, compared to pure metal–O_2 batteries, metal–O_2/CO_2 batteries generally exhibit lower energy efficiency because the formed carbonate products are wide bandgap insulators that require a lot of energy to decompose. In fact, O_2 can be considered a pollutant in the strictly metal–CO_2 electrochemistry, but to achieve metal–air batteries that can be responded to in a real environmental atmosphere, the role of O_2/CO_2 should not be ignored. Tremendous efforts have been made over the last few years to understand the fundamental reactions of these complex systems, but considerable controversy remains, particularly in Na–O_2/CO_2 system. Constructing special catalysts can inhibit carbonate product formation or promote their decomposition, thus reducing the decomposition overpotential and improving energy efficiency. Another way to improve energy efficiency is to find new chemical pathways, such as constructing reversible electrochemical reactions between carbonate products and carbon species, that is, CO_2 batteries, which will be discussed in the next section.

2.2.2. Reactions in Pure Carbon Dioxide

It is the first rechargeable Na–CO_2 battery at room temperature that was proposed in 2016 by Hu et al.,[11] who used Na foil as the anode, a multi-walled carbon nanotube (MWCNT) as the catalytic cathode materials, and 1 M $NaClO_4$ in TEGDME as the aprotic electrolyte. The MWCNT has a three-dimensional porous structure, strong electrical conductivity, and superior electrolyte wettability, while the selected TEGDME is stable to sodium, has low volatility, and high sodium ion conductivity,

enabling the batteries to exhibit excellent electrochemical performance. The excellent performance of the battery is closely linked to its ability to be reversible during operation, following Equation (5).

$$4\,Na + 3\,CO_2 \leftrightarrow 2\,Na_2CO_3 + C \qquad (5)$$

From the theoretical perspective, the Gibbs free energy value of Equation (5) under standard conditions can be calculated to be −905.6 kJ mol^{-1}, which is negative, indicating that the electrochemical reaction can occur spontaneously, and the reaction could be used for electrochemical energy storage.[60] According to the isothermal relation of Gibbs free energy and electromotive force: $\Delta_r G^{\Theta} = -nFE$, the discharge voltage can be calculated to be 2.35 V, thus suggesting that the Na-CO_2 battery system is the thermodynamic possibility. Therefore, various representations had been carried out to clarify the reversible reaction mechanism (**Figure 4**a–f). The reversibility of Na_2CO_3 was confirmed by several electrochemical methods, such as in situ Raman, XRD, and XPS. The reversibility of amorphous carbon also was observed by EELS and TEM by using silver nanowire cathodes. Furthermore, by using a portable CO_2 analyzer to track the gas released during the charging process, it was observed that the CO_2 release rate was consistent with the theoretical value based on Equation (5), verifying the reversibility of the CO_2. In addition, the battery pre-filled with Na_2CO_3 and amorphous C cathodes, compared to that with pure Na_2CO_3 cathodes, showed a lower charging voltage, demonstrating that amorphous C has a beneficial effect on decreasing the reaction barrier, in favor of promoting the degradation of Na_2CO_3 during charging, further demonstrating the reversible reactivity of Na_2CO_3/carbon. Additionally, the physical evolution of polycrystalline Na_2CO_3 and carbon was observed with the aid of TEM, SAED, and EDS tests.

Further to confirm the charging mechanism of the Na–CO_2 batteries, reversible consumption of Na_2CO_3 at the cathode and quantitative deposition of sodium metal at the anode have been investigated. A Na–CO_2 battery with sodium-free architecture was reported by Sun et al. by using Super P/Al as the anode and prefilled Na_2CO_3 and CNTs as the cathode.[50] The authors optimized the Na_2CO_3 and CNTs ratio to guarantee efficient electron transport and strong reactivity, allowing the breakdown of Na_2CO_3 and CNTs to occur below 3.8 V. Subsequently, they studied the evolution of Na_2CO_3/CNT during the charging process by in situ Raman, which showed not only a gradual decrease in the main peak corresponding to Na_2CO_3 but also a gradual decrease in the intensity of the G- and D-bands relating to CNTs (Figure 4g). They monitored the gas generation using gas chromatography (GC), which showed that CO_2 was produced throughout the charging process. Confirmation of the composition of the electrolyte after charging by ^{1}H and ^{13}C nuclear magnetic resonance spectroscopy revealed that the electrolyte did not decompose and that CO_2 was not generated by side reactions. They visualized sodium production on the anode during charging by SEM and in situ optical microscope (Figure 4h). Thanks to the Super P/Al anode with a low nucleation barrier for Na plating, dendrite-free Na could be deposited quantitatively. In situ ETEM was also used to monitor Na–CO_2 battery for uncovering its electrochemical products and
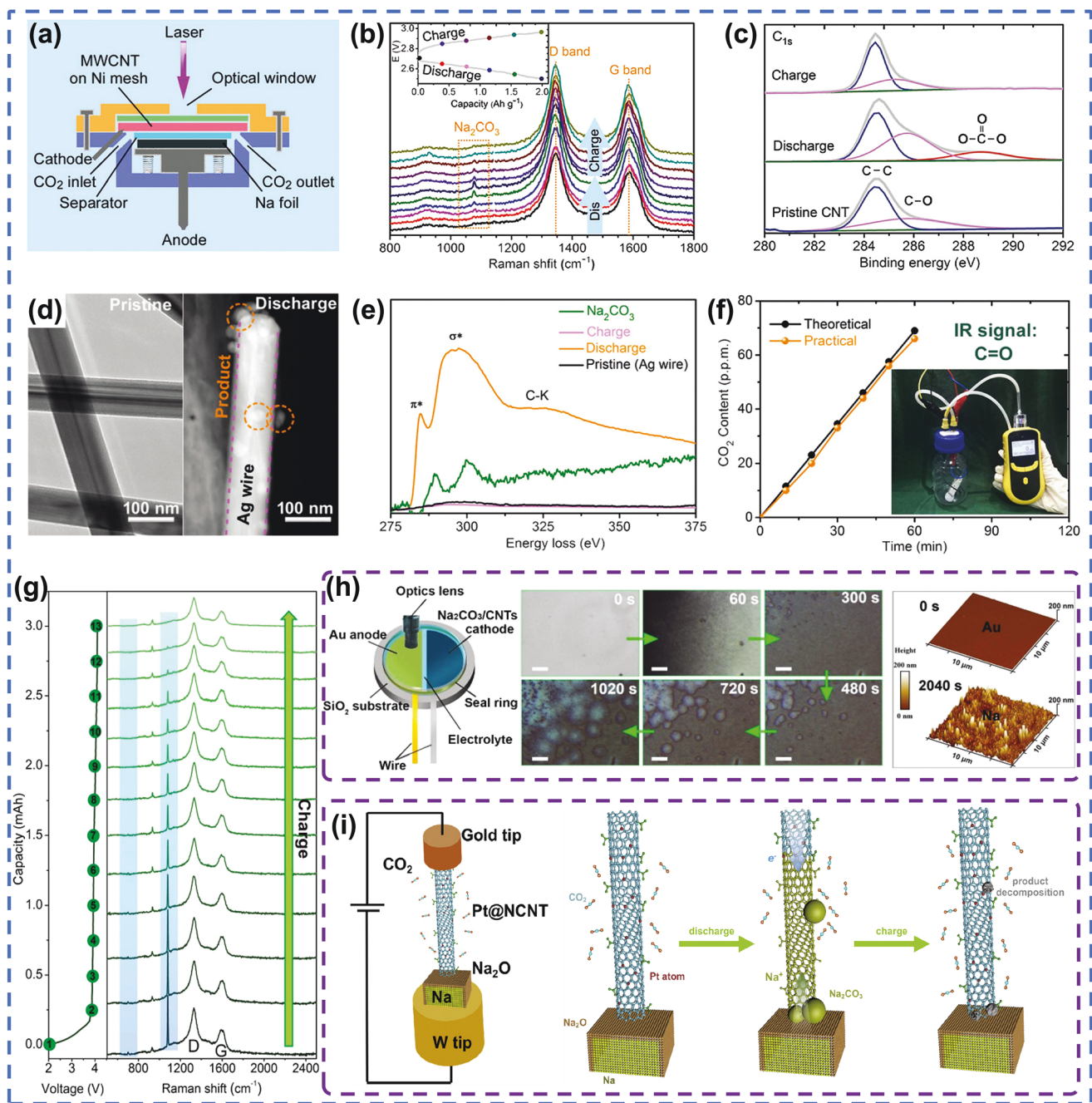
Figure 4. Reaction confirmation of $4Na + 3CO_2 \leftrightarrow 2Na_2CO_3 + C$. a) Design of in situ Raman battery. b) In situ Raman spectra and corresponding discharge/charge profiles. c) XPS. d) TEM images of pristine and discharged Ag wire. e) EELS of Ag wire cathode at different states. f) Online CO_2-evolution test. a–f) Reproduced with permission.[11] Copyright 2016, Wiley-VCH. g) The galvanostatic charge curve at 0.1 mA cm^{-2} and corresponding in situ Raman spectra. h) Schematic diagram of in situ optical microscope setup, in situ optical images of Na formation, and atomic force microscope (AFM) images of Na deposition. g,h) Reproduced with permission.[50] Copyright 2018, American Association for the Advancement of Science. i) Schematic of constructed Na–CO$_2$ nanobattery in ETEM and the discharge/charge electrochemical processes. Reproduced with permission.[29] Copyright 2020, Elsevier.

exploring its reversibility (Figure 4i).[29] A Na–CO$_2$ nanobattery was fabricated in a CO$_2$ atmosphere employing a Pt@NCNT cathode. During discharging, Na$_2$CO$_3$ spheres developed on the surface of the Pt@NCNT cathode. Whereas during charging, the Na$_2$CO$_3$ spheres decomposed into Na metal and CO$_2$. The results of this study afford an in-depth insight into the working
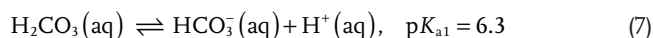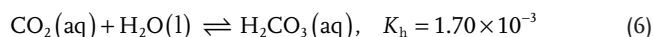
mechanism of Na–CO$_2$ batteries, encouraging us to design environmentally beneficial catalysts and Na–CO$_2$ batteries.

Based on the above studies, the detailed discharge reaction mechanism can be described as follows: In the anode chamber, metal Na is oxidized to Na$^+$ during discharge, which migrates to the cathode chamber, while CO$_2$ is reduced at the
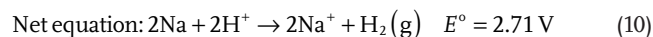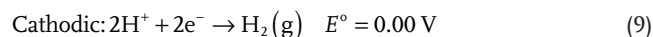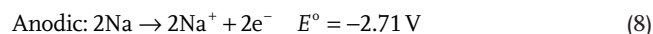
ADVANCED
SCIENCE NEWS
www.advancedsciencenews.com

NANO · MICRO
small
www.small-journal.com

cathode, which combines with the metal Na^+ from the anode to form Na_2CO_3 and reduced carbon. Conversely, during the subsequent charging process, a reversible reaction takes place whereby Na_2CO_3 combines with carbon, releasing Na^+, electrons, and CO_2, followed by the migration of Na^+ back and electrodeposition on the anode.

## 2.3. Discharge–Charge Mechanisms of Hybrid Na–CO$_2$ Batteries

Kim et al.[13] demonstrated a hybrid Na–CO$_2$ cell with metallic sodium as fuel at the anode, carbon dioxide as feedstock gas at the cathode, and a NaOH solution as the aqueous cathode solution. The sodium metal anode was maintained in an organic electrolyte, separating it from the aqueous electrolyte with a NASICON membrane. The authors suggested that CO$_2$ spontaneously dissolved to acidify the aqueous solution (Equations (6) and (7)), and then a hydrogen evolution reaction (HER) occurred during discharging, producing hydrogen and electrical energy (Equations (8)–(10)). As the potential of the cathode reaction was closely influenced by the pH of the aqueous solution, thus the kinetics of HER was accelerated by the spontaneous dissolution of CO$_2$ (**Figure 5**a,b). The H$_2$ gas generated during discharge was naturally removed at the electrode surface, so that the oxygen evolution reaction (OER) of H$_2$O oxidation occurred (Figure 5c) during charging without CO$_2$ production (Equation (11)). The chemical reaction for the dissolution of CO$_2$ is described as follows:

$$CO_2(aq) + H_2O(l) \rightleftharpoons H_2CO_3(aq), \quad K_h = 1.70 \times 10^{-3} \quad (6)$$

$$H_2CO_3(aq) \rightleftharpoons HCO_3^-(aq) + H^+(aq), \quad pK_{a1} = 6.3 \quad (7)$$

Upon discharge, the electrochemical reactions are as follows:

$$\text{Anodic: } 2Na \rightarrow 2Na^+ + 2e^- \quad E^\circ = -2.71\,V \quad (8)$$

$$\text{Cathodic: } 2H^+ + 2e^- \rightarrow H_2(g) \quad E^\circ = 0.00\,V \quad (9)$$

$$\text{Net equation: } 2Na + 2H^+ \rightarrow 2Na^+ + H_2(g) \quad E^\circ = 2.71\,V \quad (10)$$

Upon charge, the cathodic electrochemical reaction is as follows:

$$2H_2O \rightarrow O_2(g) + 4H^+ + 4e^- \quad E^\circ = 1.229\,V \quad (11)$$
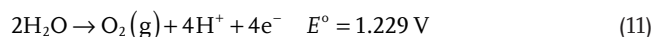
This system presented stable discharge and charge plateaus and a stable cycle of 700 h, clearly demonstrating rechargeability (Figure 5d–f). Apparently, the essence of the cell reaction is HER and OER, and CO$_2$ is not involved in the electrochemical process. Analogous reaction processes have been found in Al (Zn)–CO$_2$[61] or membrane-free Mg–CO$_2$ batteries,[62] that is, H$_2$(g) production on discharge and O$_2$/Cl$_2$(g) production on charge (Figure 5g). In fact, the practical efficiency of the CO$_2$ conversion in this process is very low, only 47.7% was obtained by the authors.[13] Nevertheless, the occurrence of HER in this work facilitated the hydration of CO$_2$, demonstrating that the

additional dissolution of CO$_2$ during the discharge process was relevant for the capture and utilization of CO$_2$, but more research is needed to increase the efficiency of CO$_2$ conversion in these hybrid Na–CO$_2$ batteries.

In contrast, a reversible hybrid Na–CO$_2$ battery had been designed in our previous study,[14] in which $Na_3Zr_2Si_2PO_{12}$ solid electrolyte (NASICON), N-doped single-walled carbon nanohorns (N-SWCNH), saturated NaCl solution were used as the separator, catalyst, and cathode aqueous solution, respectively. In combination with the unique catalytic activity of N-SWCNH and the ability of aqueous electrolytes to dissolve insulating discharge products, it makes possible the low polarization and long life of hybrid Na–CO$_2$ batteries (Figure 5h,i). The results of in situ Raman spectroscopy, XRD, SEM, and energy dispersive X-ray analyzer demonstrated that CO$_2$ was electrochemically reduced during the discharge to produce C and Na$_2$CO$_3$. The generated Na$_2$CO$_3$ is further combined with H$_2$O and CO$_2$ to produce NaHCO$_3$ (Figure 5j,k). Furthermore, a comparison experiment of Na$_2$CO$_3$ electrodes with/ without carbon sources was also carried out to verify the reaction pathway of Na$_2$CO$_3$ decomposition, proving the importance of carbon involvement in reducing the reaction potential of Na$_2$CO$_3$ decomposition. The reversible deposition of Na in hybrid Na–CO$_2$ batteries was also demonstrated with nickel foam as the anode and Na$_2$CO$_3$/N-SWCNH as the cathode. Regrettably, the gas evolution was not confirmed in this work, and further efforts are still needed.

Currently, hybrid Na–CO$_2$ batteries are still a relatively new field of research. Indeed, different aqueous electrolytes matched with different catalysts will give rise to different CO$_2$ reduction mechanisms, as it allows for flexible conversion of CO$_2$ to various value-added chemicals by means of a proton-coupled electron transfer mechanism.[15,33] For example, Yang et al. proposed and realized a reversible hybrid Li–CO$_2$ battery with a lithium plate as the anode, a NaCl solution as the cathode solution, a solid electrolyte (LAGP) as the separator, and a bifunctional Pd-based electrocatalyst as the cathode.[63] The reaction mechanism was considered to be $CO_2 + 2Li + 2H^+ \rightleftharpoons HCOOH + 2Li^+$. The battery exhibited a high operating voltage and energy density with an outstanding selectivity of 97% for CO$_2$-HCOOH conversion. A Zn–CO$_2$ flow battery was designed that consists of a CNT cathode, a zinc anode, and a 1-ethyl-3-methylimidazolium tetrafluoroborate electrolyte, which continuously consumed CO$_2$ to produce CH$_4$ under ambient conditions with a Faraday efficiency of 94%.[64] However, the rechargeable aqueous Zn–CO$_2$ batteries with coralloid Au,[65] Ir@Au,[66] Ni atoms doped graphitic[67] produced CO, while the aqueous Zn–CO$_2$ batteries with Bi-doped carbon nanosheets,[68] Pd-based electrocatalyst[69] produced HCOOH. In addition, it is worth mentioning that the cathode CRR pathway of aqueous CO$_2$ batteries is highly correlated with the target product, which determines its discharge voltage and theoretical energy density.[70] For example, in a Zn–CO$_2$ battery with HCOOH as the discharge product, the discharge voltage is 0.95 V and the corresponding energy density is 467 Wh kg^{-1};[69] while CO as the discharge product, whose discharge voltage is 0.71 V, and the corresponding energy density is 348 Wh kg^{-1} (based on the weight of the anode and cathode reactants.[66] Overall, hybrid metal–CO$_2$ batteries can offer the possibility of developing flexible CO$_2$ electrochemistry that can simultaneously output

**ADVANCED
SCIENCE NEWS**
www.advancedsciencenews.com
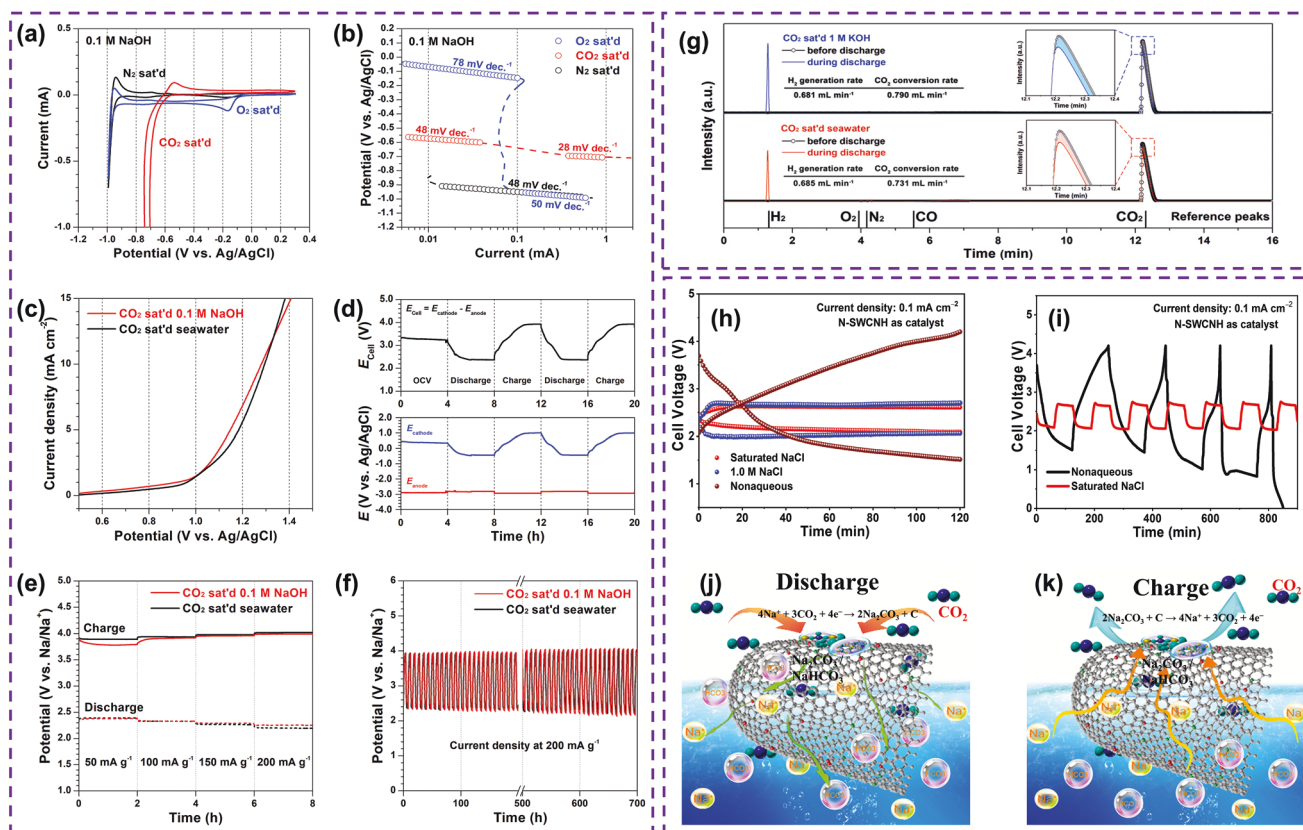
**NANO · MICRO
small**
www.small-journal.com

Figure 5. a) CV profiles and b) Tafel analysis. CV and Tafel of the half-cell configuration indicated that CO_2 dissolution in NaOH provides an electrochemically favorable environment for HER. c) Anodic rotating disk electrode profile. The oxidation curve corresponding to OER was observed near 1.0 V. Performances of hybrid Na–CO_2 cell: d) discharge–charge profiles measured in a three-electrode configuration. e) Charge–discharge profiles at different current densities and f) cycle performance. a–f) Reproduced with permission.[13] Copyright 2018, Elsevier. g) The GC profiles of outlet CO_2 feed gas before and during discharging under CO_2-saturated 1 M KOH (top) and seawater (bottom). Reproduced with permission.[61] Copyright 2019, Wiley-VCH. h) Discharge–charge voltage and i) cycling performance curves with different catholyte. j,k) Schematic of the discharge and charge processes in the hybrid Na-CO_2 battery using N-SWCNH as a catalyst and the NaCl solution as an aqueous catholyte. Reproduced with permission.[14] Copyright 2020, Elsevier.

electrical energy and produce high value-added chemicals upon discharge, while generating O_2 upon charge. In addition to the recently reported HCOOH, CO, and CH_4, the direct formation of high value-added chemicals such as CH_3OH, C_2H_5OH, and C_2H_4 in aqueous metal–CO_2 batteries is still expected, even though it is a challenging and difficult goal. In addition, the gas and liquid products enable the batteries to eliminate the accumulation of solid products.

3. Key Remaining Challenges

The basics of the Na–CO_2 battery system have progressed tremendously in the last few years (**Table 1**), but there is still much to learn to facilitate practical applications. Below, we briefly discuss the key challenges (**Figure 6**).

First and foremost, the understanding of the battery chemistry and reaction mechanism is still controversial. Some reports have identified the reaction mechanism of nonaqueous Na–CO_2 batteries by observing the discharge products (Na_2CO_3 and C),[11,23] however, there is no plausible mechanism explanation for how these systems function in a reversible manner.

It seems most studies only make mechanical or unquestioning references to the reaction mechanism, although the reaction may be central to these studies. It has been shown that the formation of $O_2^{\bullet-}$ intermediates is involved at the cathode in the presence of O_2 and that CO_2 can react with $O_2^{\bullet-}$,[16,58] making it challenging to reveal the mechanisms in these batteries using conventional analytical techniques due to the extreme sensitivity of the intermediates. Therefore, it is necessary to further understand the mechanisms of CO_2/O_2 reduction, Na_2CO_3 nucleation, and growth. Furthermore, owing to the decomposition reactions of Na_2CO_3 and C products involving the more complex four-electron transfer, thus the origin of the low overpotential during discharge and charge needs to be clarified to gain insight into CRR and CER. Similarly, the reaction mechanism in the field of hybrid Na–CO_2 batteries research is still a mystery. There is a need to clarify the type of reaction product, to fully determine the presence or absence of carbon-containing chemicals and H_2 release, and to factor in the charge overpotential associated with the proton-coupled charge transfer of the CO_2 reduction mechanism.

The current anode material is mainly sodium metal, which is promising to achieve high energy densities at the battery level

Table 1. Some typical achievements for Na–CO_2 batteries in terms of functional materials and electrochemical properties.

Working conditions (battery type, atmosphere, anode)	Electrolyte	Cathode materials	Voltage gap, applied current	Full discharge capacity, current density	Cyclability	Ref.
Aprotic, CO_2/O_2 (2:3)	0.75 M $NaCF_3SO_3$/IL	Super P	≈0.5 V	3500 mAh g^{-1}, 70 mA g^{-1}	–	[16]
Aprotic, pure CO_2	0.75 M $NaCF_3SO_3$/IL	Super P	–	183 mAh g^{-1}, 70 mA g^{-1}	–	[16]
Aprotic, CO_2/O_2 (3:2)	1 M $NaClO_4$/TEGDME	Super P	–	2882 mAh g^{-1}, 70 mA g^{-1}	–	[16]
Aprotic, pure CO_2	1 M $NaClO_4$/TEGDME	Super P	–	173 mAh g^{-1}, 70 mA g^{-1}	–	[16]
Aprotic, CO_2/O_2 (1:1)	SiO_2-IL-TFSI/PC-NaTFSI	Porous carbon	≈2.2 V, 200 mA g^{-1}	–	≈20 cycles with the cut-off capacity of 800 mAh g^{-1} at 200 mA g^{-1}	[41]
Aprotic, CO_2/O_2 (1:1)	SiO_2-IL-TFSI/PC-NaTFSI	Nickel foam	≈3 V, 200 mA g^{-1}	≈3.5 mAh	100 cycles with a limited capacity of 200 mAh $g_{cathode}^{-1}$ at 50 µA cm^{-2}	[53]
Aprotic, pure CO_2	1 M $NaClO_4$/TEGDME	TEGDME-treated MWCNT (t-MWCNT)	≈1.00 V, 1000 mA g^{-1}	60 000 mAh g^{-1}, 1000 mA g^{-1}	200 cycles with a limited capacity of 2000 mAh g^{-1} at 1000 mA g^{-1}	[11]
Aprotic, pure CO_2	1 M $NaClO_4$/TEGDME	Ru@KB	≈1.5 V, 100 mA g^{-1}	11 537 mAh g^{-1}, 100 mA g^{-1}	130 cycles with a limited capacity of 1000 mAh g^{-1} at 200 mA g^{-1}	[22]
Aprotic, pure CO_2	1 M NaTFSI/TEGDME	Ru@CNT	≈1.5 V, 100 mA g^{-1}	20 277 mAh g^{-1}, 100 mA g^{-1}	100 cycles with a limited capacity of 500 mAh g^{-1} at 100 mA g^{-1}	[23]
Aprotic, pure CO_2	1 M $NaClO_4$/TEGDME	CMO@CF	≈2.0 V, 200 mA g^{-1}	8448 mAh g^{-1}, 200 mA g^{-1}	75 cycles with a limited capacity of 500 mAh g^{-1} at 200 mA g^{-1}	[26]
Aprotic, pure CO_2	1 M $NaClO_4$/TEGDME	CO@CF	≈2.1 V, 200 mA g^{-1}	7427 mAh g^{-1}, 200 mA g^{-1}	≈46 cycles with a limited capacity of 500 mAh g^{-1} at 200 mA g^{-1}	[26]
Aprotic, pure CO_2	1 M $NaClO_4$/TEGDME	MO@CF	≈2.2 V, 200 mA g^{-1}	6634 mAh g^{-1}, 200 mA g^{-1}	≈44 cycles with a limited capacity of 500 mAh g^{-1} at 200 mA g^{-1}	[26]
Aprotic, pure CO_2	1 M $NaClO_4$/TEGDME	MoS_2/SnS_2	≈1 V, 50 mA g^{-1}	35 889 mAh g^{-1}, 50 mA g^{-1}	100 cycles with a restricted capacity of 500 mAh g^{-1} at 50 mA g^{-1}	[28]
Aprotic, pure CO_2 (sodium-fluorinated graphene anode)	0.5 M $NaCF_3SO_3$/TEGDME	Carbon cloth-supported δ-MnO_2 electrodes	≈1.5 V, 200 mA g^{-1}	–	391 cycles with a limited capacity of 1000 mAh g^{-1} at 200 mA g^{-1}	[45]
Aprotic, pure CO_2	1 M $NaClO_4$/TEGDME	RuO_2@a-MWCNTs	≈1.2 V, 100 mA g^{-1}	–	120 cycles with a limited capacity of 500 mAh g^{-1} at 100 mA g^{-1}	[71]
Aprotic, pure CO_2	1 M $NaClO_4$/TEGDME	$ZnCo_2O_4$@CNT	≈1.8 V, 100 mA g^{-1}	12 475 mAh g^{-1}, 100 mA g^{-1}	150 cycles with a limited capacity of 500 mAh g^{-1} at 100 mA g^{-1}	[72]
Flexible solid-state, pure CO_2	SPE consisting of PEO/$NaClO_4$/3 wt% SiO_2	MWCNTs@Ni	≈1.2 V, 50 mA g^{-1}	–	240 cycles with a limited capacity of 500 mAh g^{-1} at 50 mA g^{-1}	[12]
All-solid-state, pure CO_2 (compact NaF-rich interphase on Na surface)	SN-based electrolyte	MWCNTs	≈1.53 V, 50 mA g^{-1}	7624 mAh g^{-1}, 50 mA g^{-1}	100 cycles with a limited capacity of 1000 mAh g^{-1} at 200 mA g^{-1}	[24]
All-solid-state, pure CO_2	Polymer electrolyte of PEO-$NaClO_4$/glass fiber matrix	NC900	≈1.5 V, 100 mA g^{-1}	10 500 mAh g^{-1}, 100 mA g^{-1}	320 h (80 cycles) with a limited capacity of 1000 mAh g^{-1} at 500 mA g^{-1}	[25]
Quasi-solid, pure CO_2 (Reduced graphene oxide Na anodes)	CPE consisting of PVDF-HFP-4% SiO_2/$NaClO_4$-TEGDME	TEGDME activated MWCNT (a-MCNTs)	≈1.75 V, 500 mA g^{-1}	5000 mAh g^{-1}, 50 mA g^{-1}	400 cycles with a limited capacity of 1000 mAh g^{-1} at 500 mA g^{-1}	[30]
Quasi-solid-state, pure CO_2	NASICON, gel electrolyte	Co-NCF	≈1.75 V, 0.1 mA cm^{-2}	1777 mAh g^{-1} at 0.5 mA cm^{-2}	367 cycles at 0.1 mA cm^{-2}	[73]
All-solid-state, pure CO_2	NASICON electrolyte	Succinonitrile-treated Ru/CNTs	≈1.3 V, 50 mA g^{-1}	28 830 mAh g^{-1}, 100 mA g^{-1}	70 cycles with a limited capacity of 500 mAh g^{-1} at 50 mA g^{-1}	[32]
Hybrid, pure CO_2	0.1 M NaOH solution, NASICON	Pt/C + IrO_2 catalyst	≈1.5 V, 0.1 mA cm^{-2}	–	700 h at a current density of 200 mA g^{-1}	[13]
Hybrid, pure CO_2	Saturated NaCl solution, NASICON	SWCNHS	≈0.49 V, 0.1 mA cm^{-2}	2293 mAh g^{-1} at 0.2 mA cm^{-2}	300 cycles at 0.1 mA cm^{-2}	[14]

Table 1. Continued.

Working conditions (battery type, atmosphere, anode)	Electrolyte	Cathode materials	Voltage gap, applied current	Full discharge capacity, current density	Cyclability	Ref.
Hybrid, pure CO_2	"Water-in-salt" and NASICON	Ru@carbon current collector	≈1.65 V at a limited capacity of 500 mAh g^{-1}	–	75 cycles (50 days) with a limited capacity of 500 mAh g^{-1}	[31]
Hybrid, pure CO_2	Saturated NaCl solution, NASICON	Co/Co$_9$S$_8$@SNHC	≈0.65 V, 0.2 mA cm^{-2}	18.9 mAh cm^{-2} (≈7421 mAh g^{-1}) at 0.5 mA cm^{-2}	200 cycles at 0.1 mA cm^{-2}	[42]
Hybrid, pure CO_2	Saturated NaCl solution, NASICON	Fe-Cu-N-C	≈0.44 V, 0.05 mA cm^{-2}	8411 mAh g^{-1} at 0.5 mA cm^{-2}	1550 cycles at 0.2 mA cm^{-2}	[43]
Hybrid, pure CO_2	Saturated NaCl solution, NASICON	CCO/PPy	≈0.6 V, 0.1 mA cm^{-2}	31.4 mAh cm^{-2} (≈9815 mAh g^{-1}) at 0.5 mA cm^{-2}	410 cycles at 0.2 mA cm^{-2}	[44]

because of its inherently high specific energy (1160 mAh g^{-1}) and low negative potential (–2.714 V vs standard hydrogen electrode).[48,74] Nevertheless, being a highly reactive chemical, sodium metal may rapidly react with crossover O_2, CO_2, H_2O molecules, some organic solvents, and electrolyte additives, which inevitably leads to reduced coulombic efficiency (CE) and loss of energy density.[75] In addition, upon discharge, the metallic sodium is oxidized to Na$^+$, and electrons are released; while Na$^+$ ions are reduced via an electron transfer pathway during charging (Na ↔ Na$^+$ + e$^-$). The process of Na$^+$ ion reduction to Na during charging is more complex compared to the oxidation of sodium metal during discharge. The formation of

undesirable sodium dendrites during charging has been one of the most serious issues to overcome, as sodium dendrites have the potential to penetrate the separator and thereby cause short circuits and security risks to the battery. This is, of course, a persistent drawback of various sodium metal batteries.[76–79]

In Na–CO_2 batteries, the electrolyte is used to deliver sodium ions, dissolve CO_2 and transfer it to the reaction site (nonaqueous and aqueous electrolytes), and protect the metal sodium anode (solid-state electrolyte for hybrid and solid-state Na–CO_2 batteries). Although the search for stable electrolytes has been ongoing since the inception of alkali metal ion batteries, the harsh O_2/CO_2 environment of Na–O_2/CO_2 and
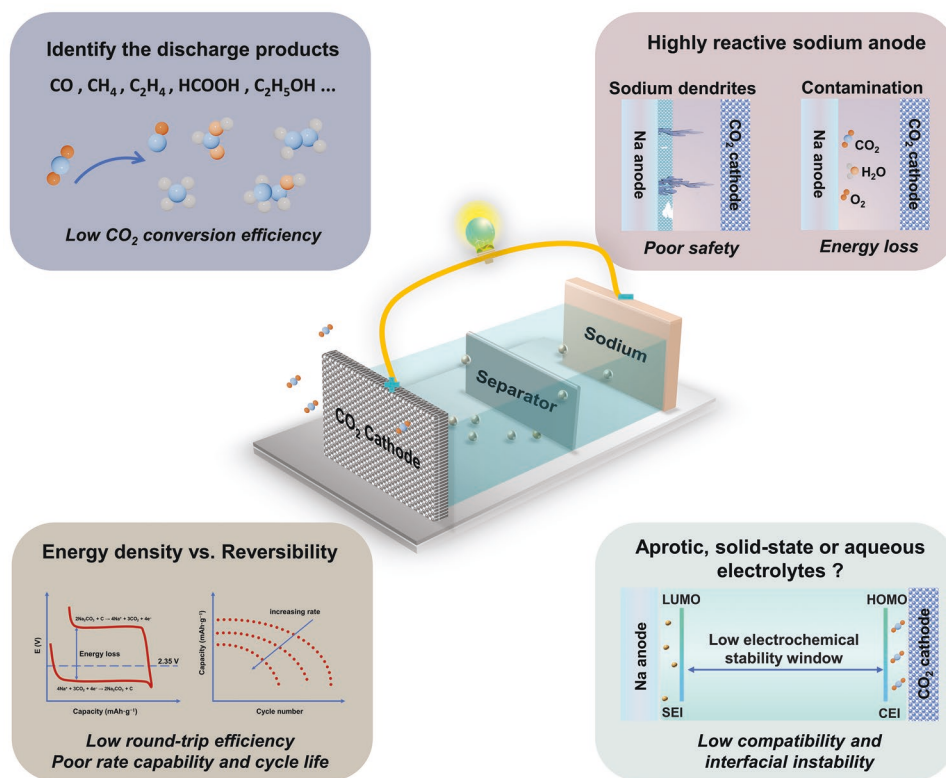

Figure 6. The main challenges for the development of Na–CO_2 batteries.

ADVANCED
SCIENCE NEWS
www.advancedsciencenews.com

NANO · MICRO
small
www.small-journal.com

Na–CO_2 batteries has led to increasingly stringent requirements for electrolytes. For the case of aprotic electrolytes, the instability of the electrolyte system is one of the major obstacles limiting the development of Na–O_2/CO_2 and Na–CO_2 batteries, given that they play a critical role in O_2/CO_2 solubility, the formation pathway of discharge products (Na_2O_2, Na_2CO_3, etc.) and the formation of the SEI layer, especially when exposed to highly reactive oxygen species.[16,41] Not all electrolytes that are available for metal–ion batteries are compatible with metal–O_2/CO_2 batteries. For example, carbonate-based electrolytes have proven unsuitable for maintaining reversible metal–O_2/CO_2 batteries due to their extreme susceptibility to nucleophilic attack by superoxide or peroxide.[80,81] In addition, the degradation or volatilization of electrolytes can seriously affect the performance of the battery and may even induce early cell death. Although a variety of electrolytes have been widely used, no fully stable electrolyte can meet the complex requirements of Na–O_2/CO_2 batteries. For solid-state electrolytes, polymer-based composites and ceramic-based electrolytes (NASICON) are currently used for Na–CO_2 batteries. In general, the ionic conductivity of solid electrolytes is lower than that of liquid electrolytes, which still has difficulties in meeting the requirements of high ionic conductivity, good stability, and low cost. Moreover, the structural compatibility and interfacial instability of metal anode/solid-state electrolyte/catalytic cathode materials have always been the main research direction to inhibit solid-state Na–CO_2 batteries.[51] In the case of aqueous electrolytes, the solvent (H_2O) may participate in the electrochemical process as a reactant, or HER may occur, which will reduce the specific energy density of the battery.[69] In addition, the stability of NASICON in aqueous electrolytes and electrochemical stability windows also needs to be considered.

The cathode is the main site, where the capture of CO_2 and the formation and decomposition of discharge products take place, involving a multiphase interface and complex charge transfer reactions. Typically, the electrochemical reactions of CO_2 take place at a three-phase contact interface involving the CO_2 molecules (gas), the electrolyte (liquid), and the catalytic electrode (solid). The transport of electrons and masses (e.g., Na^+ and CO_2) needs to be of sufficiently high efficiency for high performance in Na–CO_2 batteries to be possible. However, the electrochemical reactions of CO_2 in current Na–CO_2 batteries remain sluggish owing to a couple of obstacles. First, a crucial element determining the rate of the discharge/charge process is the transport of Na^+ ions and CO_2 gas through the electrolyte and cathode pores.[42] The inherent low electron conductivity of cathode materials and their limited porosity for ion and molecular transport results in poor cell rate performance. Second, CO_2 is known to be the most oxidized form of carbon, with an oxidation state of +4 and an extremely strong chemical bond of C = O (750 kJ mol^{-1}),[82] making it extremely difficult to reduce CO_2 to other carbon-containing chemicals. Moreover, CO_2 electrochemical reactions are stepwise reactions with the possibility of involving intermediates such as $O_2^{\bullet-}$, $CO_4^{\bullet-}$, $C_2O_6^{2-}$, solvated and adsorbed species,[16,58] especially aqueous Na–CO_2 batteries with very complex products.[83,84] It is difficult to regulate the complex reaction pathways and intermediates, causing slow electrochemical kinetics of the overall CO_2 electrochemical reaction. Third, in the typical nonaqueous Na–CO_2

batteries, the sluggish kinetics of the reaction between the CRR formed by Na_2CO_3 and the CER decomposed by Na_2CO_3 results in a deviation from the discharge and charge curves of the battery, giving rise to a low round-trip efficiency.[42,43] It is crucial to note that the solid Na_2CO_3 hardly dissolves in nonaqueous aprotic electrolytes but accumulates in the cathode. The poor electron transfer and ionic diffuse characteristics of solid Na_2CO_3 are significant hurdles to attaining superior CRR and CER rates.[42,43]

4. Strategies for Na–CO_2 Batteries Toward Practical Applications

4.1. Na Anodes Protection

The safety of sodium metal anodes has been an important concern for high-energy-density sodium metal batteries. However, the cycle stability and efficiency of Na–CO_2 batteries are far from satisfactory so far. Besides the endless dendrite growth, volume changes, and the instability in the electrolyte to which all sodium metal anodes are exposed during the repeated stripping/plating process in comparison to conventional sodium ion secondary batteries, the stability of sodium anodes is affected by more factors in Na–CO_2 batteries, especially in oxygen-involved Na–O_2/CO_2 batteries.[85] For example, the commonly utilized glass fiber separators are unable to prevent the crossover of contaminants, such as oxygen-related species, H_2O, CO_2, and redox mediators shuttling. The complex internal environment and electrochemical processes endow sodium metal anodes with additional challenges. Consequently, effective protection strategies must be developed to strengthen the performance of Na–CO_2 batteries. In this section, we shed light on the efforts made in the field of Na–CO_2 batteries in terms of interfacial modification and electrolyte engineering, and electrode design, aiming to enlighten the future design of stable sodium-metal anodes for high-performance Na–CO_2 batteries.

Several strategies have been proposed to defeat the notorious parasitic reactions between reactive metallic sodium and electrolyte components, the crossover of pollutants such as O_2, H_2O, CO_2, and the formation of sodium self-dendrites (**Figure 7**a). The first one is artificial interphase engineering, aiming to inhibit the formation of sodium dendrites and the side reactions during the process of cycling (Figure 7b). The second is the use of alternative sodium metal anodes, such as sodium-free anodes or sodium-containing composite anodes, which can avoid the formation of sodium dendrites (Figure 7c). The third is to create solid-state or quasi-solid-state electrolytes for suppressing side reactions and sodium dendrite penetration through the separator (Figure 7d), which will be discussed in the electrolyte section.

4.1.1. Artificial Interphase Engineering

The natural SEI layer is produced by the spontaneous interaction of the highly reactive metallic sodium anode with the electrolyte/gas.[77,86] The SEI layer acts as a protective interface separating the metallic sodium anode from the electrolyte,
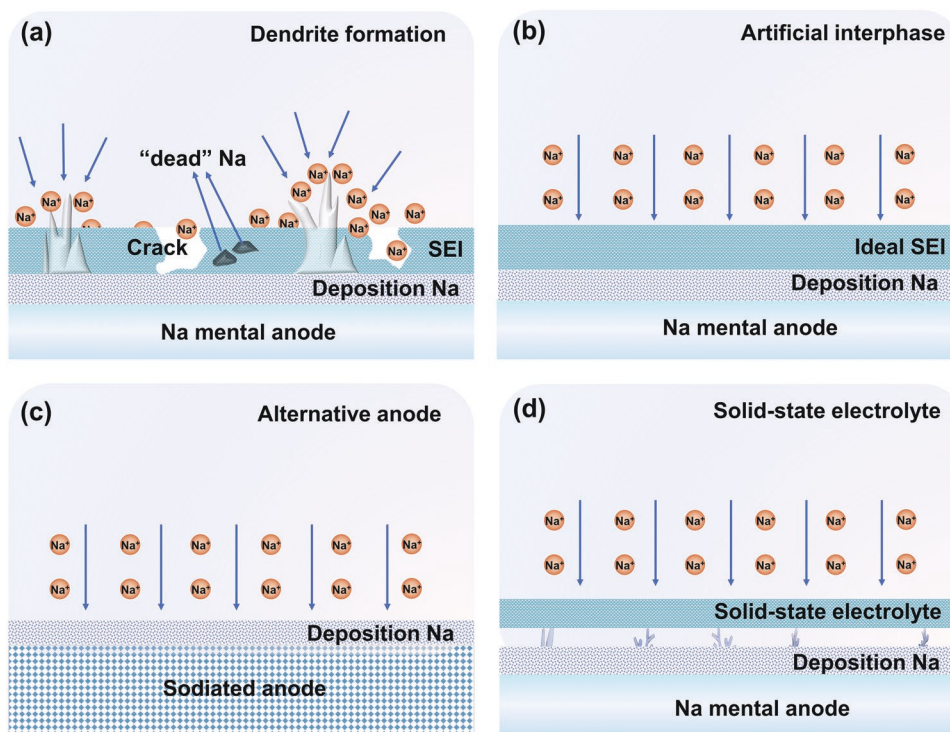
ADVANCED
SCIENCE NEWS
www.advancedsciencenews.com

NANO · MICRO
small
www.small-journal.com

Figure 7. Schematic representation of the problems and solution strategies for sodium metal anodes, a) sodium dendrite formation, b) artificial interphase engineering, c) alternative sodium metal anodes, and d) insertion of solid-state or quasi-solid-state electrolytes.

preventing further corrosion of the sodium metal to some extent. Unfortunately, uneven Na ion flux and repetitive volume change during Na metal plating/stripping cause cracking and collapse of the natural SEI layer.[76] The localized and enhanced sodium ion flux near cracks will aggravate the growth of dendrites, which continuously consume electrolytes and regenerates thick SEI with poor conductivity and massive sodium dendrites, leading to low CE and short cycle life. Meanwhile, the sodium dendrites are easily separated from the anode surface during the sodium stripping process and become "dead" sodium by the SEI isolation,[86] which increases the cell impedance and results in low CE, severe polarization, and rapid capacity degradation (Figure 7a). Furthermore, the uncontrolled growth of sodium dendrites can pierce the separator and contact the cathode material of the battery, leading to safety issues such as short circuits and thermal runaway.

The ideal SEI layer should have chemical and electrochemical stability, high sodium ion conductivity, sufficient density, small thickness, and good flexibility to mechanically inhibit sodium dendrite growth.[87] The use of specific organic solvents, sodium salts, and additives to create a stable artificial SEI layer in situ is effective in stabilizing the sodium-metal interface and increasing the performances of $Na–CO_2$ and $Na–O_2/CO_2$ batteries. Lu et al. designed a dense NaF-rich interface on the Na surface through a chemical process involving fluoroethylene carbonate-Na^+ and Na metal (**Figure 8**a).[24] The in situ formed NaF-rich interface consists of organic and inorganic species (e.g., NaF, RONa, RCO_2Na, $ROCO_2Na$) with a thickness of about 8 nm, exhibiting a low interfacial resistance and excellent mechanical properties. The dense NaF-rich interface not

only protects the succinonitrile (SN)-based electrolyte from side reactions with metallic Na anode but also allows for modulating the homogeneous deposition of dendrite-free Na. After cycling at 0.1 mA cm^{-2} for 4000 h, the assembled symmetric cell exhibited a low overpotential of 150 mV. Furthermore, the all-solid-state $Na–CO_2$ cell, which used a modified Na anode, SN-based solid-state electrolyte, and MWCNT cathode, exhibited a large discharge specific capacity (7624 mAh g^{-1}) and great cycling stability (100 cycles).

Recently, Mao et al. constructed a stable NaF-rich SEI layer to inhibit sodium dendrite growth.[45] The SEI layer was achieved by combining a modest quantity (≈3 wt%) of fluorinated graphene (FG) with the native sodium through simple repetitive adsorption, folding, and hammering steps to obtain a homogeneous Na/FG composite anode. The addition of FG was critical in preserving the stability of Na/FG since the composition of the Na/FG electrode remained essentially unchanged after 16 h of air exposure. Their investigation indicated that the interaction between Na and FG occurs spontaneously and Na + FG → NaF + graphene is thermodynamically feasible. The formation of a strong SEI layer, which is critical for increasing the electrochemical and mechanical stability of Na/FG electrodes, is driven by NaF and graphene. As shown in the in situ optical micrograph (Figure 8b), the sodium dendrites on bare Na grew fast and even reached the counter electrode. In contrast, there was no significant dendritic formation for the Na/FG electrode. The Na/FG surface tended to maintain its uniformity, and the Na/FG electrode exhibited low voltage hysteresis and long cycle life. Ultimately, a stable cycle of 391 cycles was achieved by the $Na–CO_2$ battery with Na/FG anode.
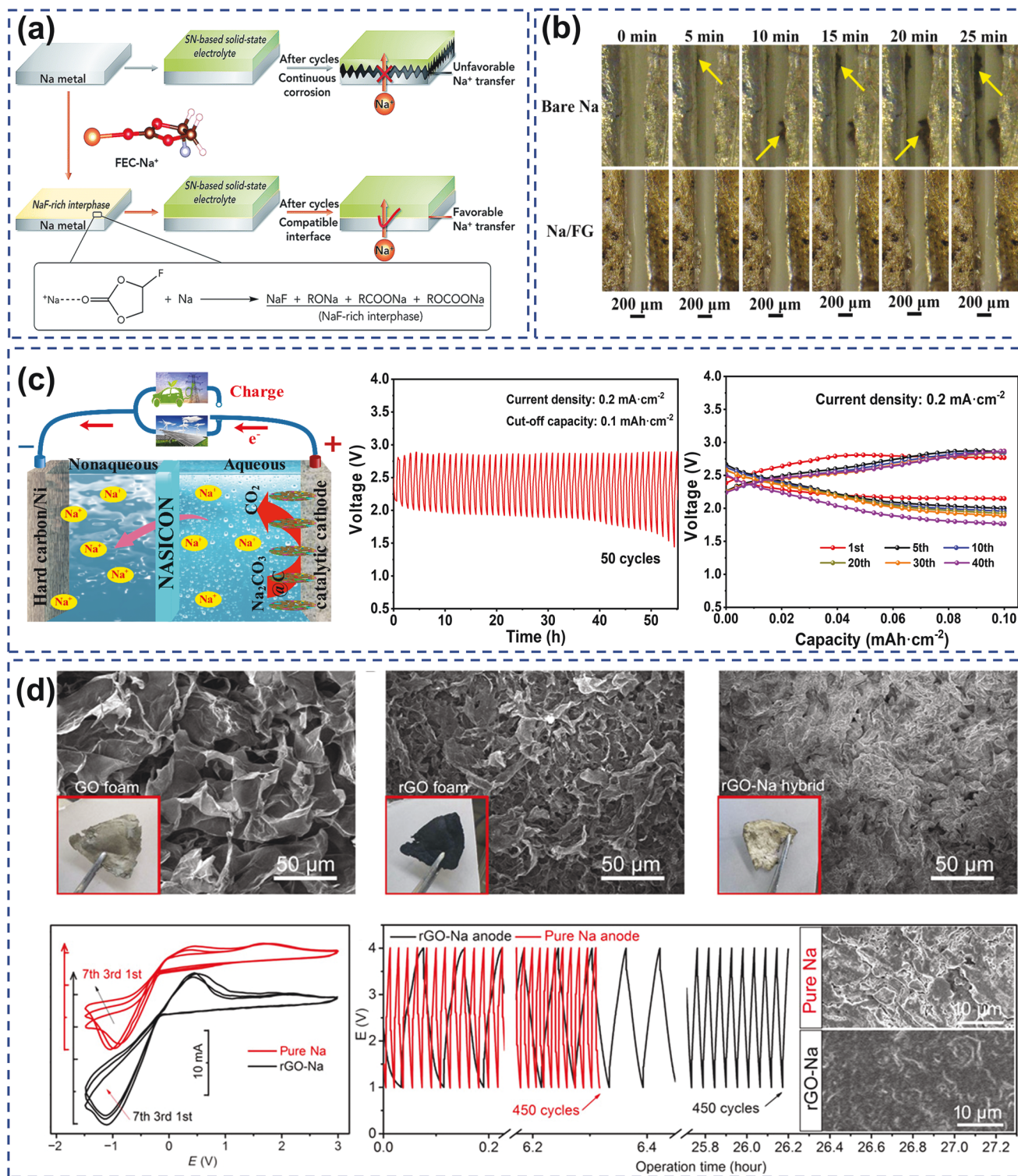
ADVANCED
SCIENCE NEWS

www.advancedsciencenews.com

NANO · MICRO

small

www.small-journal.com

Figure 8. a) Schematic illustration of the compatibility between different Na metals and SN-based electrolytes: pristine Na metal and 1 M NaClO$_4$/FEC modified Na metal. Reproduced with permission.[24] Copyright 2019, Royal Society of Chemistry. b) In situ optical microscopy images of Na deposition on bare Na and Na/FG electrodes. Reproduced with permission.[45] Copyright 2021, Wiley-VCH. c) Schematic diagram of hybrid Na–CO$_2$ battery charging from Na$_2$CO$_3$@C catalytic cathode and its cycling performance and selected discharge–charge curves. Reproduced with permission.[42] Copyright 2020, Elsevier. d) SEM images and photographs of GO foam, rGO foam reduced by molten Na, and rGO-Na anode surface; CVs of Na$^+$ plating/stripping; fast discharge/charge profiles of quasi-solid-state Na–CO$_2$ batteries in Ar atmosphere and corresponding SEM images of rGO-Na and pure Na anode surfaces after 450 cycles. Reproduced with permission.[30] Copyright 2017, American Association for the Advancement of Science.

ADVANCED
SCIENCE NEWS
www.advancedsciencenews.com

NANO · MICRO
small
www.small-journal.com

4.1.2. Alternative Sodium-Containing Anodes

To solve the critical problems associated with sodium dendrite growth, an additional strategy is to seek alternative anodes instead of the sodium metal anodes, such as sodium-free anodes or sodium-containing composite anodes. A hybrid Na–CO_2 battery has been reported, which uses the replacement of sodium metal with hard carbon/Ni, and the composite of Na_2CO_3, conductive carbon, and catalyst as the cathode.[42] A low charging voltage of 2.68 V was observed in the hybrid Na–CO_2 battery with the sodium-free anode, corresponding to a narrow charge–discharge overpotential gap. However, its cycling performance was limited due to the unoptimized anode interface, with only about 50 cycles at a limited capacity of 0.1 mAh cm^{-2} (Figure 8c). Similarly, a pouch-type Na–CO_2 battery employing a super P/Al anode was proposed and exhibited a satisfying energy density of 183 Wh kg^{-1} with prefilled Na_2CO_3 and CNTs as the cathode.[50]

To achieve a highly stable Na-based anode, Hu et al. constructed a reduced graphene oxide Na anode (rGO-Na) to substitute pure metallic sodium anode by infusing molten sodium into a well-affinity rGO foam (Figure 8d).[30] Compared with the pure metallic sodium, the rGO-Na anode not only had better mechanical strength and toughness but also exhibited faster Na^+ plating/stripping kinetics. More importantly, the rGO-Na inhibited the formation of Na dendrites by allowing homogeneous plating of Na^+ on the anode. The rGO-Na surface was even smoother than its initial state after 450 cycles of rapid discharge and charging under the Ar atmosphere. In contrast, serious cracks appeared on the pure Na surface after 450 cycles. The assembled coin-type Na–CO_2 cell delivered a stable cycle of 400 cycles, and the pouch-type cell also exhibited an impressive capacity (1.1 A h^{-1}), a generous energy density (232 Wh kg^{-1}), and stable cycle life (50 cycles).

4.2. Stabilize Electrolyte

The selection of a suitable electrolyte is a challenging issue for Na–CO_2 batteries because the electrolyte interacts with all three major components, anode, separator, and CO_2 cathode. In addition to safety and environmental concerns, the electrolyte controls many intrinsic parameters, such as ionic conductivity and CO_2 solubility, which largely determine the mechanism of cathode operation. As discussed in the mechanism section, the electrochemical mechanism of Na–CO_2 batteries differs for different systems. Although various electrolytes have been widely used, no completely stable electrolyte can meet the complex requirements of batteries. It is generally the lowest unoccupied molecular orbital (LUMO) and the highest occupied molecular orbital (HOMO) that determines the electrochemical stability window of an electrolyte.[88,89] In practice, the LUMO energy of the anode is higher than that of the electrolyte (salt, solvent, polymer, etc.), leading to irreversible reduction of these components and the formation of SEI on the anode.[89] A cathode electrolyte interface layer is also formed between the discharge products (NaO_2 and/or Na_2O_2, Na_2CO_3), CO_2, and the electrolyte on the cathode material.[21] The following characteristics should be present in an ideal Na–CO_2 battery electrolyte: i) Wide electrochemical stability window, zero decomposition during the operating period; ii) high CO_2 solubility and low viscosity to support rapid mass transfer; iii) high chemical and electrochemical stability in CO_2-rich environments; iv) a stable SEI layer toward the sodium metal anode to ensure long-term cycling; and v) low volatility, non-toxicity, and non-flammability. Focused on the electrolytes for applications in Na–CO_2 batteries, advancements and currently experiencing issues, including non-aqueous aprotic, aqueous, polymeric solid/quasi-solid electrolyte, and inorganic ceramic solid electrolyte (NASICON), are summarized and discussed in this section to facilitate better and more efficient Na–CO_2 electrolyte design (**Figure 9**).

4.2.1. Aprotic Electrolytes

In the past few years, the optimization of aprotic electrolytes has been studied in terms of solvents, metal salt, and additives.[89,90] Functional additives in electrolytes have aroused considerable research interest since they have the potential to boost battery performance significantly. Archer's group adopted SiO_2 nanoparticles and ionic liquid (IL) 1-methyl-3-propylimidazolium bis(trifluoromethanesulfone)imide (TFSI) as additives into a PC electrolyte for Na–O_2/CO_2 batteries.[41,53] The SiO_2 nanoparticles were highly functionalized by IL with 1.2 tethered ligands per nm^2 SiO_2. Despite the fact that conventional PC-based electrolytes have proven to be extremely unstable in metal–air batteries, the stability of PC-based electrolytes was significantly improved by the application of IL-tethered SiO_2 nanoparticles.[41] Because of the interaction of tethered IL with Na metal, a structurally durable and chemically stable SiO_2-particle-enriched SEI layer on the surface of the metallic Na anode successfully shields the sodium metal from excessive parasitic reactions. Consequently, the Na–O_2/CO_2 battery without the need for any catalysts or redox mediators could operate stably for more than 100 cycles.[53] In addition, taking into account the basic chemistry of O_2/CO_2 batteries, ether-based electrolytes are relatively stable for metal–O_2/CO_2 batteries, because of their low volatility and stability for superoxide anions and oxidation potentials. TEGDME has been proposed as a representative ether-based electrolyte. For Na–CO_2 batteries, there are currently two main electrolytes, one is TEGDME containing $NaClO_4$ component, while the other salt is sodium bis(trifluoromethylsulfonyl)imide (NaTFSI). However, ether-based electrolytes do not seem to be the best electrolytes because strong Lewis acid alkali metal ions (Li^+, Na^+) in solutions may interact strongly with oxygen atoms in ether molecules.[91] Consequently, a deeper insight into the decomposition mechanism of aprotic electrolytes (carbonate and ether groups) and the identification of a truly stable electrolyte is required.

4.2.2. Aqueous Electrolytes

The utilization of aqueous electrolytes in Na–CO_2 batteries appears to be a highly promising strategy for solving several challenges that arise in nonaqueous Na–CO_2 batteries, such as

ADVANCED
SCIENCE NEWS

www.advancedsciencenews.com

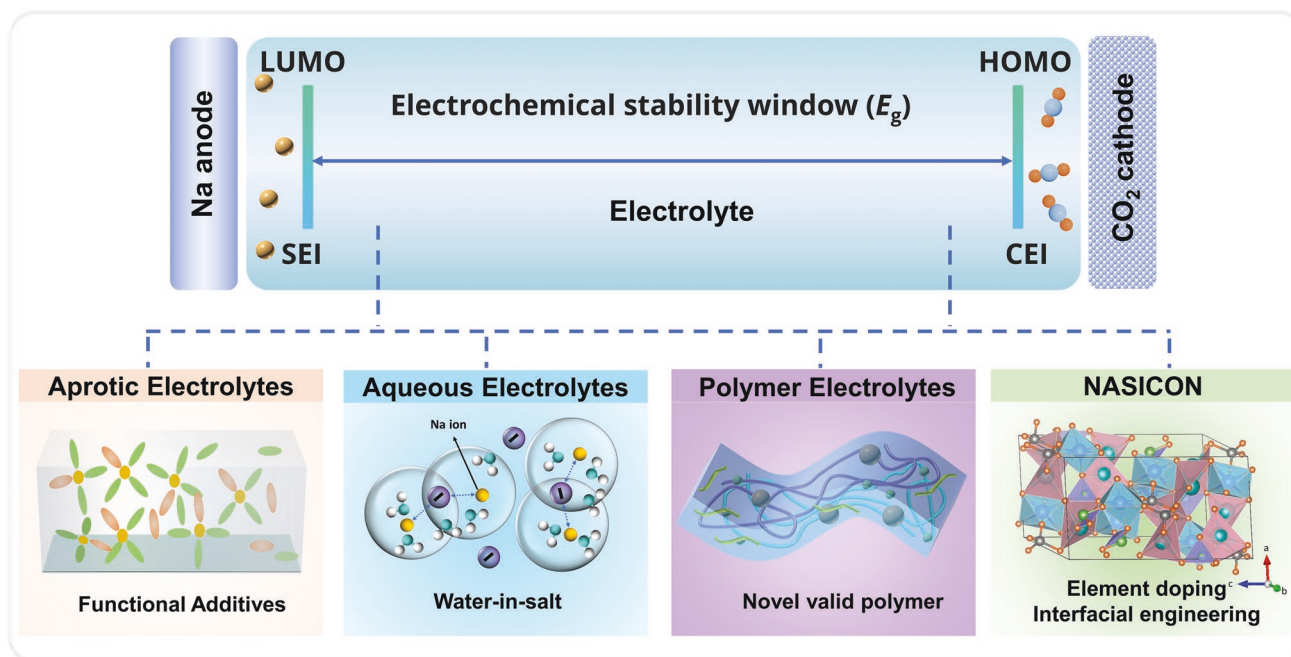NANO · MICRO
small

www.small-journal.com

Figure 9. Strategies for stabilizing electrolytes in Na–CO$_2$ batteries.

the formation of insoluble discharge products during discharge that impede CO$_2$ diffusion and lead to high overpotential and poor cycling performance. Previous studies have demonstrated that the kinetics of the discharge and charging processes are significantly enhanced in aqueous electrolytes compared to non-aqueous electrolytes, where the overpotential is much smaller than that in nonaqueous batteries.[14,92] However, in reversible hybrid Na–CO$_2$ batteries, aqueous electrolytes are currently limited to neutral or quasi-neutral solutions because NASICON separators tend to corrode in acidic solutions posing a serious safety hazard,[93] and CO$_2$ reacts with alkaline electrolytes to produce carbonates that reduce electrolyte conductivity and cathode activity. Furthermore, the application of aqueous electrolytes is restricted by their narrow potential window, and the aqueous solvent H$_2$O is involved in the reaction, inevitably minifying the energy density of the battery. The preparation of a highly concentrated electrolyte, "water-in-salt" (WiS) electrolyte, has been shown to be an effective method to reduce electrolyte-related side reactions. Kang et al. demonstrated a Na–CO$_2$ battery based on NASICON and WiS electrolyte by selecting water as the solvent with 17 м NaClO$_4$.[31] The LSV and corresponding DEMS measurements demonstrated that the evolution of H$_2$ was hindered by increasing WiS concentration (**Figure 10**a–d). Moreover, the 17 м NaClO$_4$ aqueous electrolyte showed a significantly increased electrochemical stability window of 3.45 V. The thus prepared hybrid Na–CO$_2$ batteries presented favorable discharge–charge curves during the formation and decomposition of Na$_2$CO$_3$ (Figure 10e). It is generally accepted that WiS-based low-cost hybrid Na–CO$_2$ batteries show great potential, the high concentrations of WiS electrolytes are usually accompanied by drawbacks such as high viscosity and low Na$^+$ conductivity. In addition, the stability of the solid electrolyte membrane is also critical for

performance and safety. Therefore, more efforts are needed to achieve hybrid Na–CO$_2$ batteries.

4.2.3. Polymer Electrolytes

The quasi-solid and all-solid-state polymer electrolytes (SPEs) offer opportunities to address safety concerns such as electrolyte leakage, volatilization, flammability, and savage growth of metal dendrite. Hu et al. developed a quasi-solid state composite polymer electrolyte (CEP) derived from polyvinylidene fluoride co-hexafluoropropylene (PVDF-HFP) for Na–CO$_2$ batteries.[30] This CEP exhibited high conductivity (10^{-3} S cm^{-1}), non-flammability, robust toughness, effective inhibition of electrolyte leakage, and stable electrochemical properties (**Figure 11**a). An all-solid-SPE was also used to create the flexible Na–CO$_2$ battery.[12] The SPE was composed of poly(ethylene oxide) (PEO), NaClO$_4$, and nano-SiO$_2$, where PEO not only provides a transport pathway for Na$^+$ migration through segment motion but also acts as a binder to combine sodium and CO$_2$ cathode into an integrated battery. Nano-SiO$_2$ as a filler improved the mechanical and thermal stability while reducing the crystallinity of SPE and facilitating NaClO$_4$ dissolution. The optimized SPE, which had a high sodium ionic conductivity (0.64 mS cm^{-1}) and significant ionic transference number (0.56), exhibited exceptional plating/stripping and electrochemical stability, as well as a broad electrochemical window (up to 5.5 V). The integrated flexible Na–CO$_2$ batteries showed excellent bendability ($\geq$1000 cycles) and stable operation for 80 h in bending conditions from 0° to 360° (Figure 11b). The development of bendable, foldable, and shape customizable solid-state electrolytes offers a promising direction for flexible, wear-resistant, and safe Na–CO$_2$ batteries.

**ADVANCED
SCIENCE NEWS**

www.advancedsciencenews.com
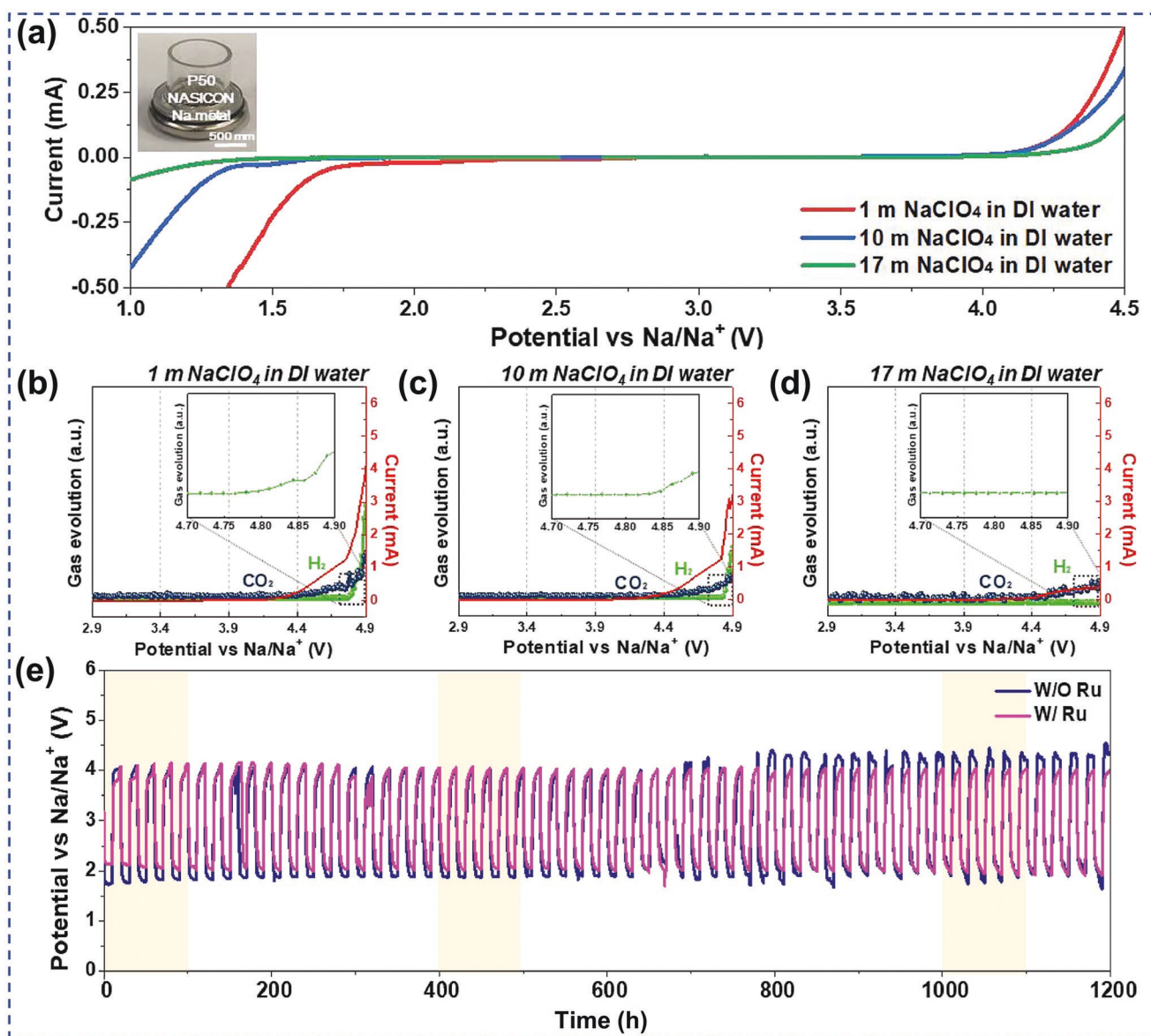
**NANO · MICRO
small**

www.small-journal.com

Figure 10. a) LSV plots of NaClO4 aqueous electrolyte solutions. The hybrid cell is photographed in the inset. b–d) LSV curves with corresponding DEMS results. e) Cycle behavior of the Na–CO2 batteries with (pink) and without (navy) Ru catalyst. Reproduced with permission.[31] Copyright 2021, Elsevier.

4.2.4. Inorganic Ceramic Solid Electrolytes

Na superionic conductor (NASICON), a sodium ion-conducting oxide ceramic with the general formula $Na_{1+x}Zr_2Si_xP_{3-x}O_{12}$ ($0 < x < 3$), is recognized for its remarkable ionic conductivity, thermal, and chemical stability.[94,95] The ion transport is caused by the hopping of Na^+ ions between the NASICON lattice gap positions,[96] which therefore allows the transport of only Na^+ cations and effectively prevents the corrosion of sodium metal by H_2O, O_2, and CO_2. Although the parasitic reaction can be partially alleviated by using solid electrolytes, low ionic conductivity and electrode/electrolyte interface problems still exist in practical applications, which can cause the rapid increase of overpotential and even premature death of Na–CO2 batteries.[95] Surface modification can effectively improve the interfacial

properties of NASICON and electrodes.[97,98] A solid-state Na–CO2 battery was fabricated using NASICON as the electrolyte with a plastic crystal interface on the cathode.[32] In situ prepared succinonitrile-based plastic crystal interphase enabled the close contact of $Na_3Zr_2Si_2PO_{12}$ with the cathode, which reduced the interfacial charge transfer resistance. The presented solid-state Na–CO2 battery delivered 50 cycles at 100 mA g^{-1} with a voltage gap of 1.4 V. Normally, one of the most effective ways of increasing the conductivity of sodium ions is element doping since it can create more vacancies or interstitials and weaken electrostatic force.[99] Lu et al. investigated magnesium-doped $Na_3Zr_2Si_2PO_{12}$ as a solid electrolyte for Na–CO2 batteries.[27] By substituting the Zr ions in $Na_3Zr_2Si_2PO_{12}$ (NZSP) with Mg ions, the ionic conductivity of $Na_{3.2}Zr_{1.9}Mg_{0.1}Si_2PO_{12}$ (NZM1SP) achieved 1.16 mS cm^{-1} at ambient temperature. The Na–CO2
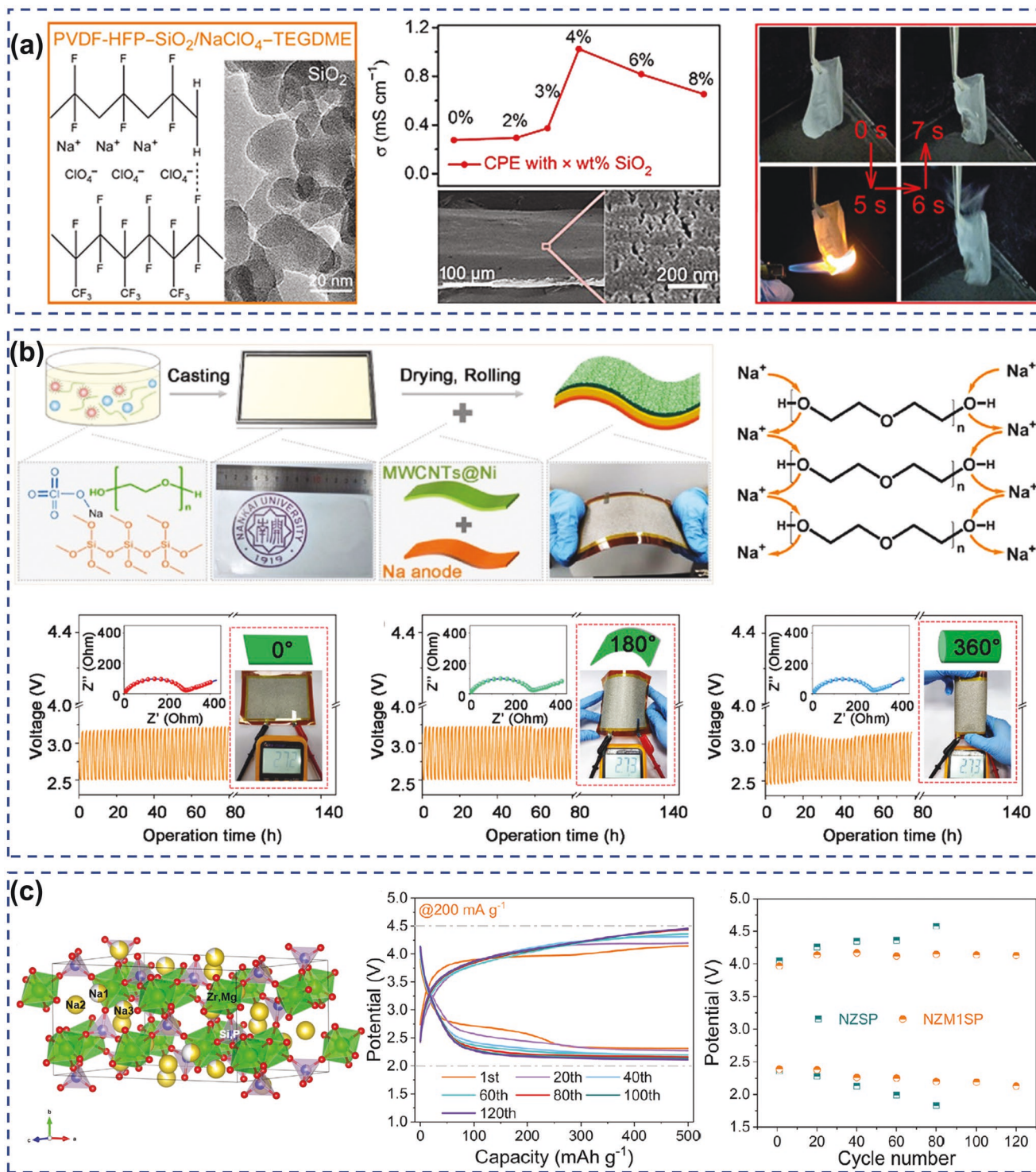
Figure 11. a) The composition, ionic conductivity, SEM image, and inflammability test of CPE. Reproduced with permission.[30] Copyright 2017, American Association for the Advancement of Science. b) Fabrication and structure of the all-solid-state integrated flexible Na–CO₂ batteries, schematic diagram of Na⁺ migration pathways in SPE, and cyclability at different bending states. Reproduced with permission.[12] Copyright 2018, Wiley-VCH. c) Simplified view of the structure of $Na_{3.2}Zr_{1.9}Mg_{0.1}Si_2PO_{12}$, charge and discharge curves, and voltage variation of the cells with NZSP-PVDF-HFP and NZM1SP-PVDF-HFP electrolytes. Reproduced with permission.[27] Copyright 2022, Wiley-VCH.

battery assembled with a composite electrolyte composed of NZM1SP and PVDF-HFP exhibited a good discharge capacity

(7720 mAh g⁻¹) and voltage gap of less than 2 V after 120 cycles (Figure 11c).

ADVANCED
SCIENCE NEWS
www.advancedsciencenews.com

NANO · MICRO
small
www.small-journal.com

4.3. Advanced CO$_2$ Electrode

One of the essential parameters for high-performance Na–CO$_2$ batteries is the development of an efficient CO$_2$ catalytic cathode that enables high activity and long-term durability. The performances that can be achieved are strongly dependent on the composition and structure of the catalytic cathode. Compared to Na–O$_2$ batteries, Na–CO$_2$ batteries are more demanding for the cathode because i) CO$_2$ is a stable linear molecule with high dissociation energy of C=O bonds (750 kJ mol^{-1}), while the dissociation energy of the O=O bond in O$_2$ is 498 kJ mol^{-1},[100] thus giving rise to difficult electroreduction of CO$_2$, a high activation barrier, large overpotential, and low conversion. ii) The decomposition of discharge product Na$_2$CO$_3$ generally involves high charging overpotential, resulting in low coulombic efficiency and even oxidative decomposition of other components.[101] For hybrid Na–CO$_2$ batteries, the discharge products can be dissolved in the aqueous catholyte, while for nonaqueous Na–CO$_2$ batteries, the gradual accumulation of Na$_2$CO$_3$ would lead to the blockage of the internal structure and passivate the active surface of the cathode materials, increasing the charge transfer impedance, and leading to increased polarization and rapid capacity decay, even to the sudden "death" of the battery.[21,42] As a consequence, the nonaqueous Na–CO$_2$ battery demand more stringent requirements for CO$_2$ cathode structure.

Generally, reactants such as Na$^+$ and CO$_2$ are required to meet on the cathode side and participate in the CO$_2$ electrochemical reaction, which must be achieved by selecting catalytic cathode materials with good electronic conductivity, fast CO$_2$, and sodium ion diffusion, and high CRR and CER catalytic activity.[42,43] It is therefore important to ensure that the cathode material features such as intrinsic conductivity, specific surface area, pore structure, the surface adsorption ability of Na$^+$ and CO$_2$ on the electrode, surface atomic structure, catalytic activity, and stability are taken into account. A porous cathode with a generous specific surface area and porosity is critical because the amount of Na$_2$CO$_3$ that can be maintained inside or on the cathode is vital to the capacity and energy density of the battery.[39,42] The increased surface area allows for more active sites in electrochemical processes, whereas a porous structure with appropriate pore sizes is necessary for mass transport and storage space for discharge products.[39,42] Catalytically active cathodes have an essential role in facilitating both CRR and CER processes by reducing the overpotential. Regulating the performance of catalytic cathodes is usually done by two strategies: i) Modulating the intrinsic electronic structure (e.g., by introducing heteroatom doping, defects, modifying the coordination state, modulating the metal active center) or ii) tuning the apparent physical structure (e.g., by modulating the nanostructure, altering the morphology, and self-supported structural design). Certainly, to attain maximum effectiveness and performance, these strategies do not need to be mutually exclusive (**Figure 12**).

4.3.1. Intrinsic Electronic Structure Modulation

The structure of cathode materials impacts the electrochemical reaction process of the battery on a variety of scales, including nano-, micro-, and macroscales.[102,103] At the nanoscale, morphology is likely to impact the local electronic structure.[103,104]
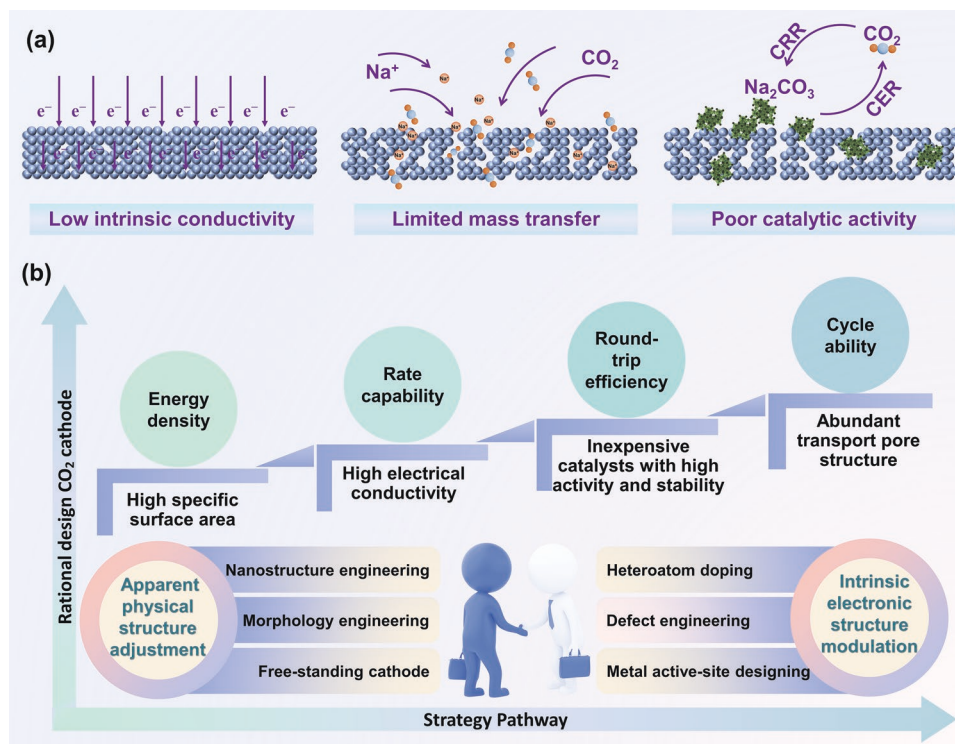

Figure 12. Summary of a) existing key issues of CO$_2$ cathode in Na–CO$_2$ batteries and b) the corresponding strategies.
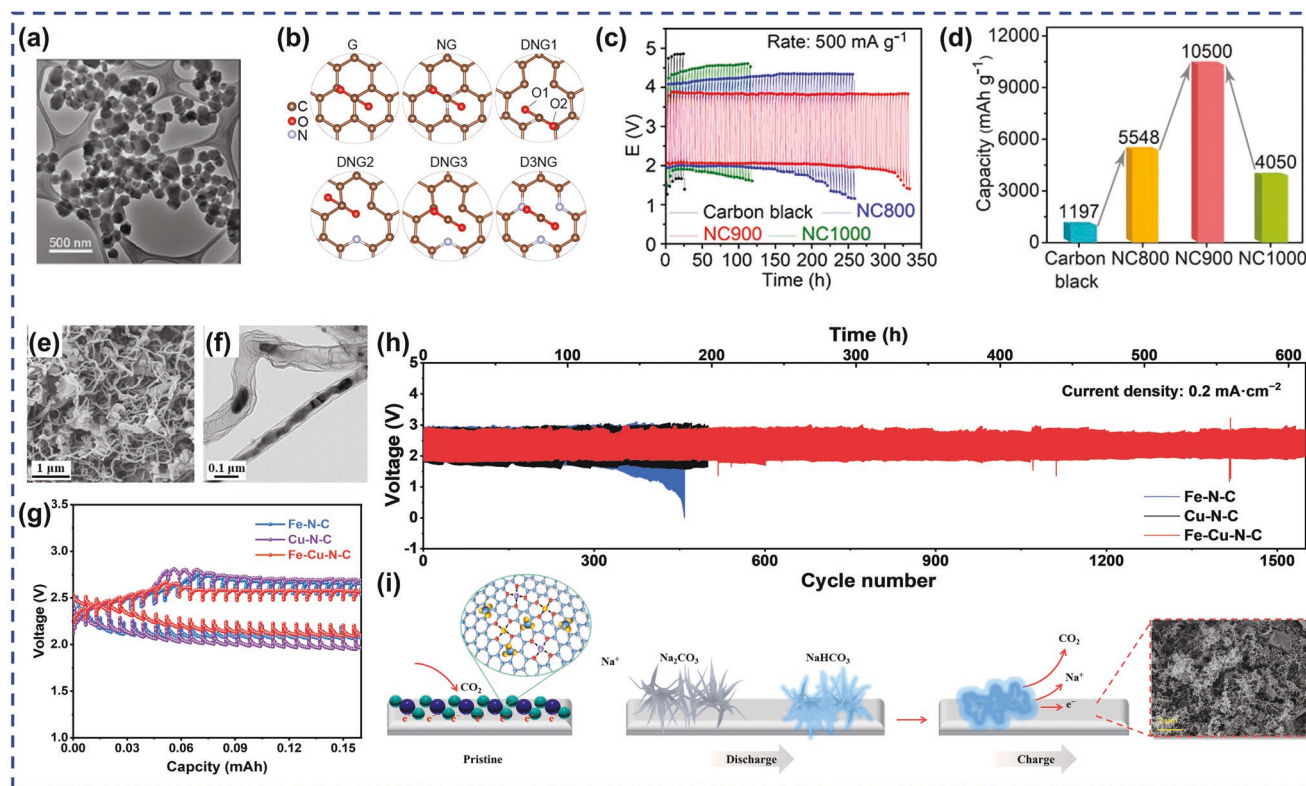
Figure 13. a) TEM image of NC900. b) CO_2 absorption models on the graphene (G), graphitic N-doped graphene (NG), and pyridinic (relaxed pyrrolic N) N-doped graphene with one N atom (DNG1-3), and three N atoms (D3NG). c) Cycling performance and d) the discharge capacity of different cathodes. a–d) Reproduced with permission.[25] Copyright 2020, American Chemical Society. e) TEM and f) TEM images of Fe-Cu-N-C. g) GITT and h) discharge–charge cycling curves of Fe-N-C, Cu-N-C, and Fe-Cu-N-C. i) An illustration of the growth and decomposition of discharge products on the Fe-Cu-N-C electrode. e–i) Reproduced with permission.[43] Copyright 2021, Royal Society of Chemistry.

At the micro- and macroscales, changing morphology potentially modifies the wettability of the electrode, ion diffusion, CO_2 transmission, Na_2CO_3 formation/decomposition, etc.[36,38] In principle, the catalytic performance of materials depends mainly on their electronic structure, and in this section, we focus on modulating the intrinsic electronic structure of the material.

Heteroatom-Doping: Several attributes of the extremely high specific surface area, rapid charge transfer, and chemical stability of carbon-based catalysts allow them to be considered potential candidates with respect to energy storage and conversion devices.[105,106] Ketjen Black (KB) and Super P are commercial carbon materials that were first exploited in CO_2 batteries,[16,58,107,108] but their poorly catalytic activity and limited structure make them more suitable for use as conductors or catalyst carriers. Carbon nanomaterials such as CNTs[11,30,50] and carbon nanohorns[14] are employed in Na–CO_2 batteries because of their unique quantum size effects and surface chemical states. Alternatively, their catalytic activity might be promoted by modifying the interfacial properties and attaching different functional groups. For example, using TEGDME-treated MWCNT materials as cathode catalysts, Na–CO_2 batteries exhibited a small voltage gap (0.6 V) and superior cyclability (200 cycles).[11] Heteroatom doping is considered to be one of the most effective strategies for tuning the electronic structure of pure carbon skeletons, which provides sufficient active sites

for CO_2 capture and utilization as well as for the generation and degradation of discharge products.[109] Of the heteroatoms (nitrogen, boron, sulfur, and phosphorus) screened so far, the most attention has been paid to nitrogen. For example, nanocarbon doped with N synthesized from zeolitic imidazolate frameworks (ZIF-8) was developed as an excellent cathode material for all-solid-state Na–CO_2 batteries.[25] The optimized N-doped nanocarbon with microporous properties exhibited high electronic conductivity (two times that of carbon black) and highly favorable binding affinities to CO_2 molecules, allowing free transfer of CO_2 during cell reaction and facilitating electrochemical progress of CRR and CER, which enables the formed thin sheetlike products to decompose more readily on charging than the bulk product. All of these advantages were combined to produce all-solid Na–CO_2 batteries that delivered low overpotential, long cycle life (320 h), a large deep discharge capacity (10 500 mAh g^{-1}), and satisfactory energy density (180 Wh kg^{-1} in a pouch cell at 50 °C) (**Figure 13**a–d). The fact that nitrogen doping is usually favorable for catalysis can be explained by: i) The electronegativity of nitrogen atoms containing lone pairs of electrons is higher than that of carbon atoms, and N doping changes the potential distribution and the electronic environment on the sp2 carbon skeleton,[105] which in turn alters the active centers of preferential adsorption and nucleation. It is, in fact, possible to easily introduce foreign atoms into the lattice of the carbon material by high-temperature treatment,

which would damage the perfect sp2 carbon lattice.[110] The presence of nitrogen atoms at the edges or in the basal plane of the carbon material matrix gives rise to different defect configurations (pyridine-N, graphite-N, pyrrole-N, etc.) and the catalytic activity is related to the structural nature and density of the nitrogen defect configuration in the material,[111] ii) carbon-based materials exhibit a reduced band gap, which is defined by their LUMO and HOMO.[112] The catalytic activity of carbon in electron transfer reactions tends to increase as the bandgap decreases. The band gap decreases as nitrogen atoms are doped into the carbon matrix, increasing the electron mobility and improving the donor–acceptor properties, consequently, higher electron mobility and lower electron work function can be achieved at the reaction interface.[37]

Defect Engineering: Defect engineering has similarities to heteroatom doping strategies in tuning the electron density and charge distribution of catalysts, which have also emerged as an appropriate strategy for adjusting the catalytic activity of materials. Defects, such as vacancies, grain boundaries, lattice distortions, edges, interfacial dislocations, etc., are often considered to be high-energy adsorption sites and active sites.[110] As a result of the presence of many uncoordinated sites and dangling bonds, they are not thermodynamically stable, which allows diffusion and electron transfer and facilitates enhanced surface catalytic activity. The introduction of defects in carbon nanomaterials also shows promise for the improved electrochemical performance of metal–CO_2 batteries.[113,114] For instance, carbon catalysts with high levels of defects are able to support the rapid formation and breakdown of discharge products, displaying enhanced electrochemical performances.[114,115] Beyond defects in carbon nanomaterials, defects in non-carbon materials are also attractive. Recently, an ultrathin MoS_2/SnS_2 nanosheet with S-vacancies was exploited as a catalyst for Na–CO_2 batteries.[28] In comparison to pristine MoS_2, the insertion of SnS_2 induces a phase conversion of MoS_2 from the 2-H phase to the 1-T phase, resulting in lower overpotential, improved cycling stability, and discharge capacities up to 35 889 mAh g^{-1}. The superior performances are due to potential changes in the local atomic environment and phase transitions, where SnS_2 doping leads to a lack of coordination of molybdenum atoms, inducing a large number of S-vacancies, activating and optimizing the 2H-MoS_2 basal planes.

Metal Active-Site Designing: Transition metal elements co-doped with nitrogen in carbon-based materials (M-N-C) are a special type of defect where metal atoms are dispersed on the surface of the carrier.[116,117] Strong interfacial interactions occur between the metal atoms and adjacent carbon and heteroatoms to form stable M–N_x moieties, whose unique coordination structure and low coordination and unsaturation coordination environment endow the metal atoms with special electronic characteristics, giving rise to extraordinary kinetic properties.[118,119] Recently, our group constructed N-doped CNT composites (Fe-Cu-N-C) with dense Fe and Cu sites by introducing Fe^{3+} and Cu^{2+} to modulate the in situ grown CNTs.[43] Fe-Cu-N-C has been demonstrated to show higher catalytic activity and durability than Cu-N-C and Fe-N-C, allowing for faster generation and degradation of discharge products as well as distinguished cycling performance of over 600 h (1550 cycles) (Figure 13e–i). As electrons tend to migrate readily from the

core metal sites to the CNTs, the presence of Fe and Cu in the CNTs may diminish the local work function of the carbon surface.[120] Furthermore, Fe and Cu combine with N to generate a large number of Fe–N_x and Cu–N_x active sites that are encased inside CNTs, thereby preventing electrolyte corrosion and ensuring stable catalytic performance throughout time.[43]

4.3.2. Apparent Physical Structure Adjustment

The apparent physical structure of cathode materials has been of considerable interest as it has a significant impact on the physical and chemical behavior of electrochemical reactants, catalysts, and products. This section focuses on the contribution of non-electrons induced by the apparent physical structure to the performance of Na–CO_2 batteries. An elaborate design for the apparent physical structure of cathode materials is anticipated to yield enhanced catalytic activity and fast reaction kinetics, improving Na_2CO_3 reversibility and reducing the overpotential of the battery.

Nanostructure Engineering: In recent years, nanomaterials have shown remarkable effects on electrocatalytic applications due to their unique bulk, surface, and quantum size properties.[121] Nano metallic and carbon composites may be more exciting types of catalysts than pure carbon-based nanomaterials. In particular, the electronic structure of metal particles can be significantly modified when the metal nanocrystal size is diminished to the atomic level, that is, the formation of individual atomically dispersed metal sites, where the metal atom utilization is maximized and the catalytic activity is highest.[122] Anchoring or compounding nano- or sub-nanostructures on a carbon substrate is an effective technique that is widely employed in the design of cathode catalysts for metal–CO_2 batteries. The noble metal ruthenium (Ru) and its oxides (RuO_2) have been proven to exhibit excellent catalytic activity in metal–CO_2 batteries. For instance, Na–CO_2 batteries fabricated with Ru nanoparticles on porous KB carbon (Ru@KB)[22] or CNT (Ru/CNT),[23] ultrafine RuO_2 nanoparticles on MWCNTs[71] were able to enhance the reversibility of the discharge product Na_2CO_3, reducing the overpotential, and providing good cycling stability and high discharge capacity. The ultimate small size of nanostructures is considered to be single atoms.[123] A Na–CO_2 nanobattery was successfully constructed using nitride and single Pt atoms doped CNT as the cathode.[29] As expected, the discharge rate was significantly improved due to the single-atom Pt catalyst. Besides precious metals, active non-precious metal nanocatalysts are ideal and efficient catalysts for CO_2 batteries. The Co/Co_9S_8 active nanoparticles, which were immobilized on S, N-codoped carbon (Co/Co_9S_8@SNHC) by a micro-mesoporous confinement synthesis strategy, had been synthesized as a catalyst for hybrid Na–CO_2 batteries (**Figure 14**a).[42] As a result of the elaborately designed microporous and mesoporous structures, the savage growth and aggregation of Co/Co_9S_8 nanoparticles were inhibited, exposing a large number of high-density active centers; while electron transmission, electrolyte permeation, and CO_2 diffusion could be accelerated, and sufficient space was available for the discharge products to be stored. The Na–CO_2 batteries with Co/Co_9S_8@SNHC delivered, as expected,
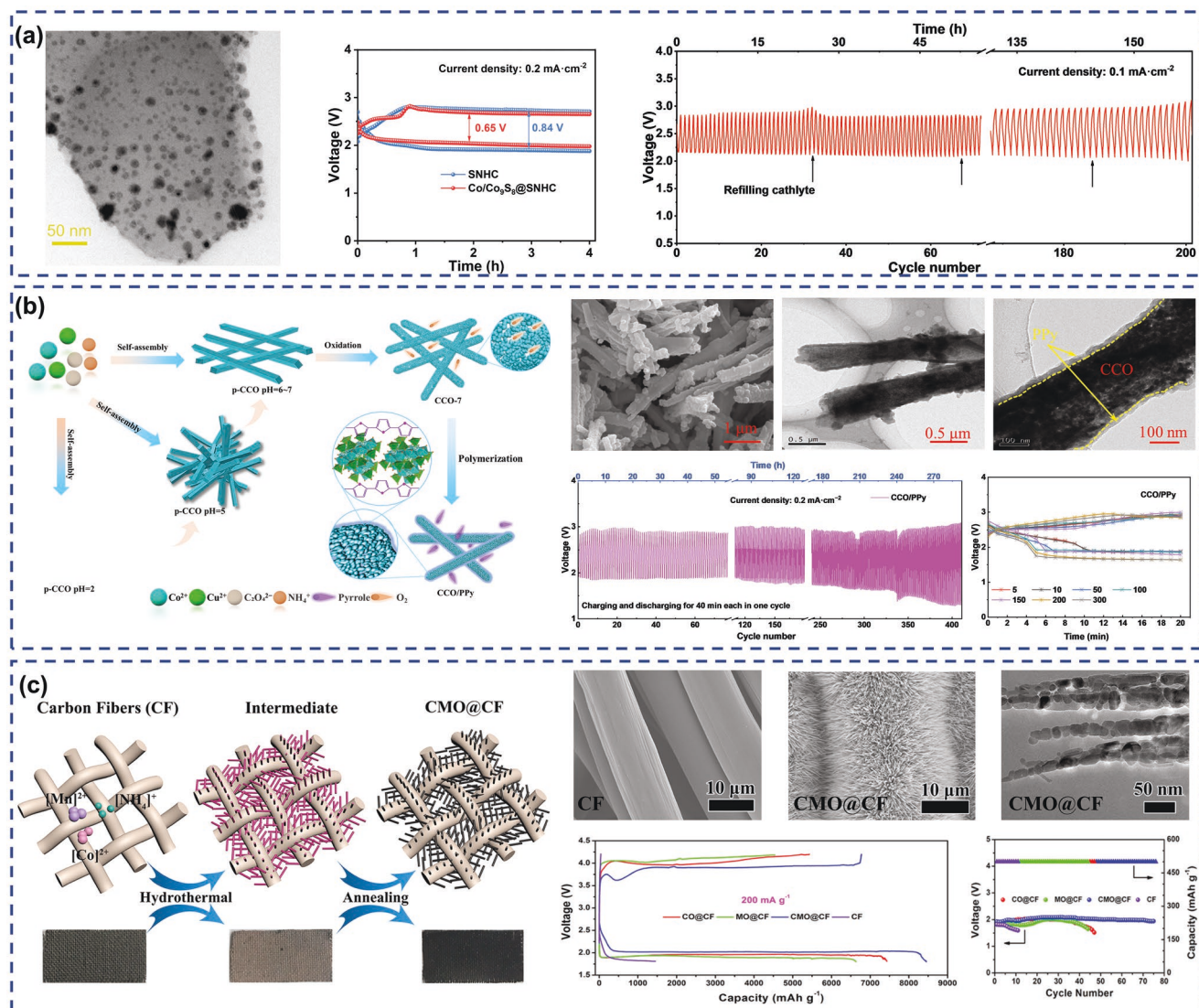
Figure 14. a) TEM image, discharge–charge voltage curves, and cycling performance of Co/Co$_9$S$_8$@SNHC. Reproduced with permission.[42] Copyright 2021, Elsevier. b) The growth mechanism, SEM and TEM images, the cycling performance, and selected discharge–charge curves of CCO/PPy. Reproduced with permission.[44] Copyright 2021, Elsevier. c) The synthesis illustration, SEM and TEM images, galvanostatic charge–discharge, and cycling curves of the CMO@CF and CF cathodes. Reproduced with permission.[26] Copyright 2018, American Chemical Society.

a narrower charge overpotential gap and a superior discharge capacity of 7421 mAh g^{-1} (vs SNHC of 6025 mAh g^{-1}). The excellent electrochemical properties were due to the synergistic combination of carbon defects, S and N dopants, and Co and Co$_9$S$_8$ nanoparticles embedded in a porous carbon matrix that supported the formation of Na$_2$CO$_3$ and its decomposition.

Morphology Engineering: Modulation of surface morphology and size may introduce new phenomena such as reconfiguration effects and even multiscale effects, which can be used to synergistically improve the performances of Na–CO$_2$ batteries. Recently, a series of morphologically controlled NH$_3$-induced self-assembly low-crystalline CuCo$_2$O$_4$ (CCO) was prepared as catalysts in hybrid Na–CO$_2$ batteries (Figure 14b).[44] It had been demonstrated that one-dimensional rod or fibrous CCO exhibited superior rate capability and lower polarization than spherical and cluster-like morphologies. Interestingly,

after polymerization of pyrrole monomers to encapsulate 1D CuCo$_2$O$_4$ in a polypyrrole shell (CCO/PPy), CuCo$_2$O$_4$ crystals underwent surface reconstruction and phase transformation into Cu$_{0.27}$Co$_{2.73}$O$_4$ with a large number of oxygen vacancies. Proper promotion of surface reconstruction of metal oxides can indeed improve catalytic performance by stimulating highly reactive metal ions and causing abundant oxygen vacancies.[124] The prepared batteries with CCO/PPy exhibited an amazing area discharge capacity (31.3 mAh cm^{-2}) and over 400 cycles.[44] The excellent performances were attributed to the modification of particle dimension and conductive polypyrrole encapsulation enhancing the ion transfer rate and electrode conductivity, moreover, the interfacial reconstruction yielded abundant oxygen vacancies and catalytically active sites.

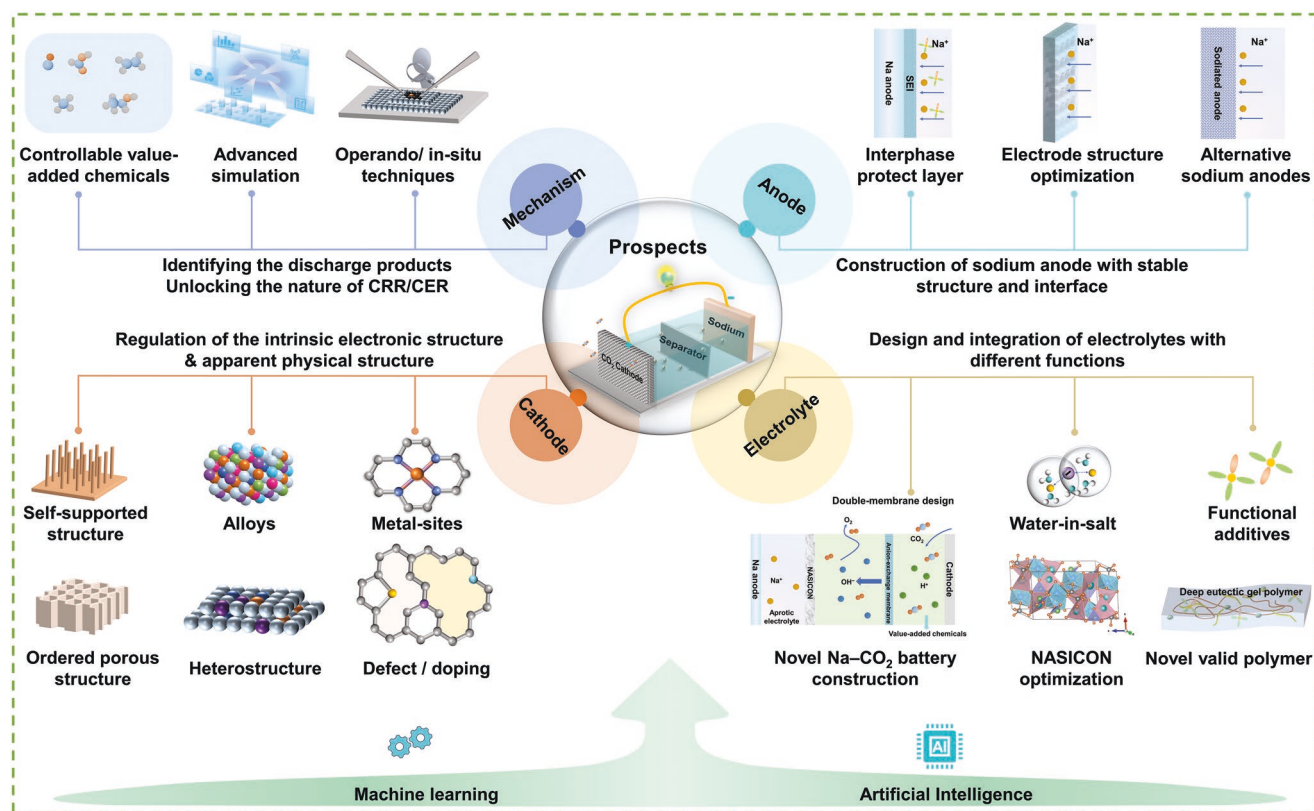*Free-Standing Cathode*: Typically, CO$_2$ cathodes prepared by the coating method, which consists of catalyst, conductive

ADVANCED
SCIENCE NEWS
www.advancedsciencenews.com

NANO · MICRO
small
www.small-journal.com

Figure 15. The schematic illustration of future research for high-performance Na–CO$_2$ batteries.

carbon, and binder, suffer from some undesirable properties such as high interfacial impedance, buried active center, low attachment of catalyst to the collector, and easy separation, as well as, the binder having the potential to cause parasitic reactions in the corrosive environment of the CO$_2$ batteries.[15] Consequently, the design of a free-standing cathode (also known as a binder-free cathode) has attracted considerable interest in avoiding these problems, ensuring adequate contact between the active center and the electrolyte, facilitating the mass transfer and charge transfer, and prolonging electrode stability and activity.[125] Fang et al. prepared a free-standing catalytic cathode (CMO@CF) by in situ growth of Co$_2$MnO$_x$ on carbon fibers (Figure 14c).[26] The designed electrode not only overcomes the drawback of poor conductivity of metal oxides but also improves the catalytic performance. The particulate Na$_2$CO$_3$ grown on the CMO@CF cathode was more readily decomposed at lower voltages than at pure cobalt oxide and manganese oxide electrodes. In addition, the Na–CO$_2$ battery based on the CMO@CF cathode exhibited excellent specific capacity (8448 mAh g^{-1}) and long-term stability (75 cycles) due to the coexistence of Co^{2+}/Co^{3+} and Mn^{2+}/Mn^{3+} redox couples.

5. Conclusion and Future Prospect

Na–CO$_2$ batteries have emerged with impressive advantages and vast potential because of their low cost, great energy density, and eco-friendliness. In this review, the advances in understanding the science of Na–CO$_2$ batteries were discussed. It first presented the fundamental properties of Na–CO$_2$ electrochemistry, and an in-depth discussion of the challenges and optimization strategies for battery configurations was provided, including the anode, electrolyte, and cathode. Considering the dilemma and further development of Na–CO$_2$ batteries, some perspectives on high-performance Na–CO$_2$ batteries are presented (**Figure 15**).

5.1. In-depth Understanding of CO$_2$ Reduction Reaction/CO$_2$ Evolution Reaction Reaction Mechanisms

The electrochemical mechanisms associated with Na–CO$_2$ batteries have been established, but they are based on the hypothesis of discharge products without in-depth experimental support. As far as the current investigation results are concerned, there do have quite a few controversies among researchers regarding the identification of the products and the basic reaction understanding during the discharge/charge process. For example, whether the discharge products are Na$_2$CO$_3$, NaHCO$_3$, Na$_2$C$_2$O$_4$, Na$_2$CO$_3$, and C, or other gaseous products is to be further confirmed; although Na$_2$CO$_3$ and C are generally accepted as the main products in nonaqueous pure Na–CO$_2$ batteries, the nucleation and growth of Na$_2$CO$_3$ with different macroscopic structures is still a puzzle. Controlling the chemical composition of the Na–CO$_2$ battery discharge products is

critical since battery performances such as capacity and energy density are defined by the type of products created during the discharge cycle, especially for hybrid Na–CO$_2$ batteries that produce value-added chemicals. In addition, the primary sources of Na–CO$_2$ electrochemical side reactions and their properties remain to be further investigated. For example, Na–CO$_2$ batteries operating properly in atmospheric environments need to account for the presence of O$_2$, and electrochemical reduction has been proven to start from O$_2$ when O$_2$ is involved in the battery. The workhorse of current computer simulations is density functional theory (DFT), yet classical DFT computations are time-consuming and costly. With the help of artificial intelligence (AI), one may capture the multi-length-scale complexity.[126–128] Machine learning (ML), as one of the major technologies for achieving AI, opens up new possibilities for product analysis, reaction identification, and prediction mechanism of Na–CO$_2$ battery.[127,129] Currently, the main experimental methods used to explore the CRR/CER mechanism of Na–CO$_2$ batteries are the ex situ characterization of CO$_2$ cathodes (XRD, SEM, Raman, TEM, XAS, XPS, etc.) before and after charge/discharge, and these ex situ methods cannot capture the important information during the actual charge/discharge process. Similarly, many other operando/in situ techniques utilized in other batteries (e.g., XRD, AFM, XPS, SEM, and XAS) should be expected to be of greater importance in the Na–CO$_2$ batteries.

5.2. Construction of Sodium Anode with Stable Structure and Interface

The application of sodium metal as a safe anode for practical Na–CO$_2$ batteries is still very challenging, especially in liquid electrolytes. The sodium metal anode is sensitive to traces of moisture and CO$_2$ in the battery environment, which increases the complexity of Na–CO$_2$ battery design. The passivation of the sodium anode lowers the discharge capacity and worsens the energy efficiency of the cell by creating an overpotential during discharge and charging, consequently, additional basic research is required to understand the processes occurring on the anode. Although sodium-metal anodes are now enjoying a renaissance and electrode design (pre-sodium composites), interface modification (artificial protective layers or surface passivation films), and electrolyte engineering have been employed to address sodium dendrite growth, infinite volume changes, and interfacial instability, the present anode protection strategies are passive and insufficient to settle all the challenges associated with sodium anode. Therefore, a comprehensive and in-depth understanding of sodium nucleation, growth, and dissolution is required, and a fundamental breakthrough may be achieved by comparing and reasonably combining various strategies through theoretical and experimental studies.

5.3. Design and Integration of Electrolytes with Different Functions

Identifying stable and efficient electrolytes is the central undertaking at this stage of Na–CO$_2$ batteries since the operating mechanism of these batteries is largely determined by the electrolyte. For aprotic electrolytes, it is necessary to discover new salts that are compatible with different solvents. In addition to low viscosity, high ionic conductivity, low volatility, safety, and low cost, which are common requirements for batteries, high CO$_2$ solubility, and the ability to be resistant to the highly oxidative environment in Na–O$_2$/CO$_2$ batteries are required. Although TEGDME ether-based electrolytes that are commonly used nowadays seem to be comparatively stable upon discharge, their electrochemical behavior (especially upon charge) is still to be thoroughly researched. Some effective strategies to alleviate the parasitic reactions of electrolytes should be considered, which include the addition of additives such as redox mediators to decrease the charge overpotential, and the application of a high concentration of salt to enlarge the voltage window of organic electrolytes, as well as through de-solvation/salting out or solubility enhancements to break the upper limit of salt solubility. Emerging deep eutectic electrolytes are also promising, but more comprehensive investigations are required.

In aqueous electrolytes, CO$_2$ electrochemistry is regulated by proton-coupled electron transfer. Although aqueous electrolytes offer excellent ionic conductivity, CO$_2$ reduction is still limited by the insufficient CO$_2$ solubility and transfer in the aqueous electrolytes and the energy density of Na–CO$_2$ batteries is capped due to the electrochemical instability of water. "WiS" electrolytes appear to overcome this challenge, but they still face practicality issues, either exacerbated by cost problems or limited cycling stability. Incorporating some hydrophilic organic or inert inorganic compounds may be a potential strategy. For example, strong H-bonds can be formed between water molecules and some highly polar aprotic solvents, which can suppress HER, broadening the electrochemical window.[130] Besides, the management of the pH and salt concentration of aqueous electrolytes and the use of hydrogel electrolytes are also effective strategies to be considered.[131] In addition to the consideration of the electrolyte itself, there is also a large potential for the construction of novel Na–CO$_2$ battery configurations. For example, the Na–CO$_2$ battery configurations with a double membrane structure have the potential to achieve the functional integration of efficient energy storage, CO$_2$ recovery, value-added chemicals and oxygen production.

Solid-state batteries are considered most appropriate for large-scale commercial applications because of their stability and low flammability. However, to make a new generation of Na–CO$_2$ batteries a reality, in addition to requiring solid-state electrolytes with suitable materials for superior ionic conductivity, a wide potential window, and chemical stability, it is crucial to ensure a smaller contact resistance at the electrode/electrolyte interface. Strategies such as using an interlayer that facilitates ion transport at the interface and designing polymer or ceramic composites that limit the growth of sodium dendrites are worthy to be intensively investigated. The electrode/electrolyte interface challenges should be thoroughly and critically evaluated; integrating theoretical calculations with experimental investigations and advanced characterization techniques will aid in the creation of novel and optimal electrolytes. Also, it is still worth developing new effective polymer electrolytes, such as deep eutectic gel polymer electrolytes.

ADVANCED
SCIENCE NEWS
www.advancedsciencenews.com

NANO · MICRO
small
www.small-journal.com

5.4. Rational Design of CO₂ Cathode

The CO$_2$ cathode is undoubtedly one of the most important factors affecting Na–CO$_2$ battery performances, as discharge products are deposited and decomposed on the cathode. Optimizing cathode design is essential to maximize CO$_2$ cathode utilization and improve battery performance. First, investigations are needed to be conducted on how the microstructure and physical properties (such as pore structure, specific surface area, electrical conductivity, active groups, etc.) of porous CO$_2$ cathodes affect the solid products and the capacity of the battery. That is, to design advanced structured freestanding CO$_2$ cathodes, such as porous nanoarray cathodes using 3D structures or catalysts loaded on 3D nanoarrays,[132,133] because it can offer sufficient space to accept the solid discharge products. Second, the intrinsic nature of catalysts must be investigated more deeply to clarify the mechanism of efficient electrocatalysts. For instance, probing what is the catalytic activity center of heteroatom-doped carbon catalysts (dopants or defects). It is necessary to integrate morphological and electronic advantages into one catalyst system to prepare efficient catalysts, elucidating the characteristics of catalyst structure evolution and failure mechanism, and establishing the fundamental relationship between catalyst composition and structure on electrochemical performance, especially cycling stability. Besides, it can combine some advanced algorithms and techniques for multi-scale modeling to explain some unusual phenomena and provide comprehensive guidance for electrode material improvement, electrolyte selection, and electrode-solution interface design. As the machinery for AI and ML matures, it will facilitate the exploration and development of functional materials to forecast the microscopic and macroscopic properties of materials and to optimize catalytic Na–CO$_2$ battery metrics.

In summary, the Na–CO$_2$ electrochemical system remains in its infancy and requires a great deal of future research. Particularly, more investigations shall be devoted to hybrid Na–CO$_2$ batteries. These are promising because of their potential applications in CO$_2$ mitigation, energy storage, and fuel production. Through continuous exploration and optimization of the anode, electrolyte, and cathode materials, we strongly believe that Na–CO$_2$ batteries have great promise for applications in the future.

Acknowledgements

Conflict of Interest

The authors declare no conflict of interest.

Keywords

[1] W. Steffen, K. Richardson, J. Rockstrom, S. E. Cornell, I. Fetzer, E. M. Bennett, R. Biggs, S. R. Carpenter, W. de Vries, C. A. de Wit, C. Folke, D. Gerten, J. Heinke, G. M. Mace, L. M. Persson, V. Ramanathan, B. Reyers, S. Sorlin, *Science* **2015**, *347*, 1259855.

[2] T. Wiedmann, M. Lenzen, L. T. Keysser, J. K. Steinberger, *Nat. Commun.* **2020**, *11*, 3107.

[3] J. D. Shakun, P. U. Clark, F. He, S. A. Marcott, A. C. Mix, Z. Liu, B. Otto-Bliesner, A. Schmittner, E. Bard, *Nature* **2012**, *484*, 49.

[4] S. Fankhauser, S. M. Smith, M. Allen, K. Axelsson, T. Hale, C. Hepburn, J. M. Kendall, R. Khosla, J. Lezaun, E. Mitchell-Larson, M. Obersteiner, L. Rajamani, R. Rickaby, N. Seddon, T. Wetzer, *Nat. Clim. Change* **2021**, *12*, 15.

[5] Y. Yang, Y. Zhang, J. S. Hu, L. J. Wan, *Acta Phys. Chim. Sin.* **2020**, *36*, 1906085.

[6] W. J. Kwak, Rosy, D. Sharon, C. Xia, H. Kim, L. R. Johnson, P. G. Bruce, L. F. Nazar, Y. K. Sun, A. A. Frimer, M. Noked, S. A. Freunberger, D. Aurbach, *Chem. Rev.* **2020**, *120*, 6626.

[7] J. Chen, H. Chen, S. Zhang, A. Dai, T. Li, Y. Mei, L. Ni, X. Gao, W. Deng, L. Yu, G. Zou, H. Hou, M. Dahbi, W. Xu, J. Wen, J. Alami, T. Liu, K. Amine, X. Ji, *Adv. Mater.* **2022**, *34*, 2204845.

[8] Z. Xie, X. Zhang, Z. Zhang, Z. Zhou, *Adv. Mater.* **2017**, *29*, 1605891.

[9] F. Cai, Z. Hu, S. L. Chou, *Adv. Sustainable Syst.* **2018**, *2*, 1800060.

[10] A. Khurram, M. He, B. M. Gallant, *Joule* **2018**, *2*, 2649.

[11] X. Hu, J. Sun, Z. Li, Q. Zhao, C. Chen, J. Chen, *Angew. Chem., Int. Ed.* **2016**, *55*, 6592.

[12] X. Wang, X. Zhang, Y. Lu, Z. Yan, Z. Tao, D. Jia, J. Chen, *ChemElectroChem* **2018**, *5*, 3628.

[13] C. Kim, J. Kim, S. Joo, Y. Bu, M. Liu, J. Cho, G. Kim, *iScience* **2018**, *9*, 278.

[14] C. Xu, K. Zhang, D. Zhang, S. Chang, F. Liang, P. Yan, Y. Yao, T. Qu, J. Zhan, W. Ma, B. Yang, Y. Dai, X. Sun, *Nano Energy* **2020**, *68*, 104318.

[15] J. Xie, Z. Zhou, Y. Wang, *Adv. Funct. Mater.* **2019**, *30*, 1908285.

[16] S. K. Das, S. Xu, L. A. Archer, *Electrochem. Commun.* **2013**, *27*, 59.

[17] S. R. Gowda, A. Brunet, G. M. Wallraff, B. D. McCloskey, *J. Phys. Chem. Lett.* **2013**, *4*, 276.

[18] M. Asadi, B. Sayahpour, P. Abbasi, A. T. Ngo, K. Karis, J. R. Jokisaari, C. Liu, B. Narayanan, M. Gerard, P. Yasaei, X. Hu, A. Mukherjee, K. C. Lau, R. S. Assary, F. Khalili-Araghi, R. F. Klie, L. A. Curtiss, A. Salehi-Khojin, *Nature* **2018**, *555*, 502.

[19] S. Xu, S. Lau, L. A. Archer, *Inorg. Chem. Front.* **2015**, *2*, 1070.

[20] H. K. Lim, H. D. Lim, K. Y. Park, D. H. Seo, H. Gwon, J. Hong, W. A. GoddardIII, H. Kim, K. Kang, *J. Am. Chem. Soc.* **2013**, *135*, 9733.

[21] N. E. Benti, G. S. Gurmesa, C. A. Geffe, A. M. Mohammed, G. A. Tiruye, Y. S. Mekonnen, *J. Mater. Chem. A* **2022**, *10*, 8501.

[22] L. Guo, B. Li, V. Thirumal, J. Song, *Chem. Commun.* **2019**, *55*, 7946.

[23] S. Thoka, C. M. Tsai, Z. Tong, A. Jena, F. M. Wang, C. C. Hsu, H. Chang, S. F. Hu, R. S. Liu, *ACS Appl. Mater. Interfaces* **2021**, *13*, 480.

[24] Y. Lu, Y. Cai, Q. Zhang, L. Liu, Z. Niu, J. Chen, *Chem. Sci.* **2019**, *10*, 4306.

[25] X. Hu, P. H. Joo, E. Matios, C. Wang, J. Luo, K. Yang, W. Li, *Nano Lett.* **2020**, *20*, 3620.

[26] C. Fang, J. Luo, C. Jin, H. Yuan, O. Sheng, H. Huang, Y. Gan, Y. Xia, C. Liang, J. Zhang, W. Zhang, X. Tao, *ACS Appl. Mater. Interfaces* **2018**, *10*, 17240.

[27] L. Lu, C. Sun, J. Hao, Z. Wang, S. F. Mayer, M. T. Fernández-Díaz, J. A. Alonso, B. Zou, *Energy Environ. Mater.* **2022**, https://doi.org/10.1002/eem2.12364.

ADVANCED
SCIENCE NEWS

www.advancedsciencenews.com

NANO · MICRO

small

www.small-journal.com

[28] K. Pichaimuthu, A. Jena, H. Chang, C. Su, S. F. Hu, R. S. Liu, *ACS Appl. Mater. Interfaces* **2022**, *14*, 5834.

[29] Y. Zhu, S. Feng, P. Zhang, M. Guo, Q. Wang, D. Wu, L. Zhang, H. Li, H. Wang, L. Chen, X. Sun, M. Gu, *Energy Storage Mater.* **2020**, *33*, 88.

[30] X. Hu, Z. Li, Y. Zhao, J. Sun, Q. Zhao, J. Wang, Z. Tao, J. Chen, *Sci. Adv.* **2017**, *3*, 1602396.

[31] E. Im, J. H. Ryu, K. Baek, G. D. Moon, S. J. Kang, *Energy Storage Mater.* **2021**, *37*, 424.

[32] Z. Tong, S. Wang, M. Fang, Y. Lin, K. Tsai, S. Tsai, L. Yin, S. Hu, R. Liu, *Nano Energy* **2021**, *85*, 105972.

[33] J. Xie, Y. Wang, *Acc. Chem. Res.* **2019**, *52*, 1721.

[34] A. Jena, Z. Tong, H. Chang, S. F. Hu, R. S. Liu, *J. Chin. Chem. Soc.* **2020**, *68*, 421.

[35] D. Sui, M. Chang, H. Wang, H. Qian, Y. Yang, S. Li, Y. Zhang, Y. Song, *Catalysts* **2021**, *11*, 603.

[36] C. Xu, X. Fang, J. Zhan, J. Chen, F. Liang, *Prog. Chem.* **2020**, *32*, 836.

[37] Z. Zhang, W. L. Bai, K. X. Wang, J. S. Chen, *Energy Environ. Sci.* **2020**, *13*, 4717.

[38] X. Sun, Z. Hou, P. He, H. Zhou, *Energy Fuels* **2021**, *35*, 9165.

[39] F. Wang, Y. Li, X. Xia, W. Cai, Q. Chen, M. Chen, *Adv. Energy Mater.* **2021**, *11*, 2100667.

[40] X. Mu, H. Pan, P. He, H. Zhou, *Adv. Mater.* **2020**, *32*, 1903790.

[41] S. Xu, Y. Lu, H. Wang, H. D. Abruña, L. A. Archer, *J. Mater. Chem. A* **2014**, *2*, 17723.

[42] C. Xu, J. Zhan, Z. Wang, X. Fang, J. Chen, F. Liang, H. Zhao, Y. Lei, *Mater. Today Energy* **2021**, *19*, 100594.

[43] C. Xu, J. Zhan, H. Wang, Y. Kang, F. Liang, *J. Mater. Chem. A* **2021**, *9*, 22114.

[44] C. Xu, H. Wang, J. Zhan, Y. Kang, F. Liang, *J. Power Sources* **2022**, *520*, 230909.

[45] Y. Mao, X. Chen, H. Cheng, Y. Lu, J. Xie, T. Zhang, J. Tu, X. Xu, T. Zhu, X. Zhao, *Energy Environ. Mater.* **2021**, *5*, 572.

[46] E. Goikolea, V. Palomares, S. J. Wang, I. R. de Larramendi, X. Guo, G. X. Wang, T. Rojo, *Adv. Energy Mater.* **2020**, *10*, 2002055.

[47] Z. Khan, M. Vagin, X. Crispin, *Adv. Sci.* **2020**, *7*, 1902866.

[48] X. Xu, K. S. Hui, D. A. Dinh, K. N. Hui, H. Wang, *Mater. Horiz.* **2019**, *6*, 1306.

[49] X. Han, X. Li, J. White, C. Zhong, Y. Deng, W. Hu, T. Ma, *Adv. Energy Mater.* **2018**, *8*, 1801396.

[50] J. Sun, Y. Lu, H. Yang, M. Han, L. Shao, J. Chen, *AAAS Res.* **2018**, *2018*, 6914626.

[51] J. Yi, S. Guo, P. He, H. Zhou, *Energy Environ. Sci.* **2017**, *10*, 860.

[52] F. Liang, Y. Sun, Y. Yuan, J. Huang, M. Hou, J. Lu, *Mater. Today* **2021**, *50*, 418.

[53] S. Xu, S. Wei, H. Wang, H. D. Abruna, L. A. Archer, *ChemSusChem* **2016**, *9*, 1600.

[54] Q. Liu, Y. Tang, H. Sun, T. Yang, Y. Sun, C. Du, P. Jia, H. Ye, J. Chen, Q. Peng, T. Shen, L. Zhang, J. Huang, *ACS Nano* **2020**, *14*, 13232.

[55] W. Zhang, Y. Huang, Y. Liu, L. Wang, S. Chou, H. Liu, *Adv. Energy Mater.* **2019**, *9*, 1900464.

[56] P. Zhang, M. Ding, X. Li, C. Li, Z. Li, L. Yin, *Adv. Energy Mater.* **2020**, *10*, 2001789.

[57] Z. Zhao, Y. Su, Z. Peng, *J. Phys. Chem. Lett.* **2019**, *10*, 322.

[58] K. Takechi, T. Shiga, T. Asaoka, *Chem. Commun.* **2011**, *47*, 3463.

[59] W. Yin, A. Grimaud, F. Lepoivre, C. Yang, J. M. Tarascon, *J. Phys. Chem. Lett.* **2017**, *8*, 214.

[60] C. Zu, H. Li, *Energy Environ. Sci.* **2011**, *4*, 2614.

[61] C. Kim, J. Kim, S. Joo, Y. Yang, J. Shin, M. Liu, J. Cho, G. Kim, *Angew. Chem., Int. Ed. Engl.* **2019**, *58*, 9506.

[62] J. Kim, A. Seong, Y. Yang, S. Joo, C. Kim, D. H. Jeon, L. Dai, G. Kim, *Nano Energy* **2021**, *82*, 105741.

[63] R. Yang, Z. Peng, J. Xie, Y. Huang, R. A. Borse, X. Wang, M. Wu, Y. Wang, *ChemSusChem* **2020**, *13*, 2621.

[64] K. Wang, Y. Wu, X. Cao, L. Gu, J. Hu, *Adv. Funct. Mater.* **2020**, *30*, 1908965.

[65] S. Gao, M. Jin, J. Sun, X. Liu, S. Zhang, H. Li, J. Luo, X. Sun, *J. Mater. Chem. A* **2021**, *9*, 21024.

[66] X. Wang, J. Xie, M. A. Ghausi, J. Lv, Y. Huang, M. Wu, Y. Wang, J. Yao, *Adv. Mater.* **2019**, *31*, 1807807.

[67] Z. Zeng, A. G. A. Mohamed, X. Zhang, Y. Wang, *Energy Technol.* **2021**, *9*, 2100205.

[68] M. Khalid, X. Zarate, M. Saavedra-Torres, E. Schott, A. M. B. Honorato, M. R. Hatshan, H. Varela, *Chem. Eng. J.* **2021**, *421*, 129987.

[69] J. Xie, X. Wang, J. Lv, Y. Huang, M. Wu, Y. Wang, J. Yao, *Angew. Chem., Int. Ed. Engl.* **2018**, *57*, 16996.

[70] S. Gao, T. Wei, J. Sun, Q. Liu, D. Ma, W. Liu, S. Zhang, J. Luo, X. Liu, *Small Struct.* **2022**, *3*, 2200086.

[71] Z. Wang, Y. Cai, Y. Ni, Y. Lu, L. Lin, H. Sun, H. Li, Z. Yan, Q. Zhao, J. Chen, *Chin. Chem. Lett.* **2022**, https://doi.org/10.1016/j.cclet.2022.04.003.

[72] S. Thoka, Z. Tong, A. Jena, T. Hung, C. Wu, W. Chang, F. Wang, X. Wang, L. Yin, H. Chang, S. Hu, R. Liu, *J. Mater. Chem. A* **2020**, *8*, 23974.

[73] B. W. Xu, D. Zhang, S. L. Chang, M. J. Hou, C. Peng, D. F. Xue, B. Yang, Y. Lei, F. Liang, *Cell Rep. Phys. Sci.* **2022**, *3*, 100973.

[74] Y. Wang, Y. Wang, Y.-X. Wang, X. Feng, W. Chen, X. Ai, H. Yang, Y. Cao, *Chem* **2019**, *5*, 2547.

[75] H. Yadegari, Q. Sun, X. Sun, *Adv. Mater.* **2016**, *28*, 7065.

[76] B. Sun, P. Xiong, U. Maitra, D. Langsdorf, K. Yan, C. Wang, J. Janek, D. Schroder, G. Wang, *Adv. Mater.* **2020**, *32*, 1903891.

[77] Y. Zhao, K. R. Adair, X. Sun, *Energy Environ. Sci.* **2018**, *11*, 2673.

[78] Q. Zhang, Z. Wang, X. Li, H. Guo, W. Peng, J. Wang, G. Yan, *Chem. Eng. J.* **2022**, *431*, 133456.

[79] Y. Dong, C. Yan, H. Zhao, Y. Lei, *Small Struct.* **2022**, *3*, 2100221.

[80] V. S. Bryantsev, V. Giordani, W. Walker, M. Blanco, S. Zecevic, K. Sasaki, J. Uddin, D. Addison, G. V. Chase, *J. Phys. Chem. A* **2011**, *115*, 12399.

[81] B. D. McCloskey, A. Speidel, R. Scheffler, D. C. Miller, V. Viswanathan, J. S. Hummelshoj, J. K. Norskov, A. C. Luntz, *J. Phys. Chem. Lett.* **2012**, *3*, 997.

[82] H. Xie, T. Wang, J. Liang, Q. Li, S. Sun, *Nano Today* **2018**, *21*, 41.

[83] B. Kumar, J. P. Brian, S. Atla, S. Kumari, K. A. Bertram, R. T. White, J. M. Spurgeon, *Catal. Today* **2016**, *270*, 19.

[84] Q. Lu, F. Jiao, *Nano Energy* **2016**, *29*, 439.

[85] S. Zhao, B. Qin, K. Y. Chan, C. Y. V. Li, F. Li, *Batteries Supercaps* **2019**, *2*, 725.

[86] T. Wang, Y. Hua, Z. Xu, J. S. Yu, *Small* **2022**, *18*, 2102250.

[87] J. L. Zhang, S. Wang, W. H. Wang, B. H. Li, *J. Energy Chem.* **2022**, *66*, 133.

[88] J. B. Goodenough, Y. Kim, *Chem. Mater.* **2009**, *22*, 587.

[89] G. G. Eshetu, M. Martinez-Ibanez, E. Sanchez-Diez, I. Gracia, C. Li, L. M. Rodriguez-Martinez, T. Rojo, H. Zhang, M. Armand, *Chem. - Asian J.* **2018**, *13*, 2770.

[90] Q. Zhang, Z. Wang, X. Li, H. Guo, W. Peng, J. Wang, G. Yan, *J. Power Sources* **2022**, *541*, 231726.

[91] D. Aurbach, B. D. McCloskey, L. F. Nazar, P. G. Bruce, *Nat. Energy* **2016**, *1*, 16128.

[92] T. Hashimoto, K. Hayashi, *Electrochim. Acta* **2015**, *182*, 809.

[93] M. Hou, T. Qu, Q. Zhang, Y. Yaochun, Y. Dai, F. Liang, G. Okuma, K. Hayashi, *Corros. Sci.* **2020**, *177*, 109012.

[94] J. B. Goodenough, H.-P. Hong, J. A. Kafalas, *Mater. Res. Bull.* **1976**, *11*, 203.

[95] Z. Jian, Y. S. Hu, X. Ji, W. Chen, *Adv. Mater.* **2017**, *29*, 1601925.

[96] J.-P. Boilot, G. Collin, P. Colomban, *J. Solid State Chem.* **1988**, *73*, 160.

[97] Z. Gao, J. Yang, H. Yuan, H. Fu, Y. Li, Y. Li, T. Ferber, C. Guhl, H. Sun, W. Jaegermann, R. Hausbrand, Y. Huang, *Chem. Mater.* **2020**, *32*, 3970.

[98] X. Wang, J. Chen, D. Wang, Z. Mao, *Nat. Commun.* **2021**, *12*, 7109.

[99] S. Chen, C. Wu, L. Shen, C. Zhu, Y. Huang, K. Xi, J. Maier, Y. Yu, *Adv. Mater.* **2017**, *29*, 1700431.

[100] A. A. Gewirth, M. S. Thorum, *Inorg. Chem.* **2010**, *49*, 3557.

[101] N. E. Benti, Y. S. Mekonnen, R. Christensen, G. A. Tiruye, J. M. Garcia-Lastra, T. Vegge, *J. Chem. Phys.* **2020**, *152*, 074711.

[102] D. Zhang, H. Zhao, F. Liang, W. Ma, Y. Lei, *J. Power Sources* **2021**, *493*, 229722.

[103] L. Li, X. Li, Y. Sun, Y. Xie, *Chem. Soc. Rev.* **2022**, *51*, 1234.

[104] R. Xu, L. Du, D. Adekoya, G. Zhang, S. Zhang, S. Sun, Y. Lei, *Adv. Energy Mater.* **2020**, *11*, 2001537.

[105] R. Paul, L. Zhu, H. Chen, J. Qu, L. Dai, *Adv. Mater.* **2019**, *31*, 1806403.

[106] C. Hu, Y. Xiao, Y. Zou, L. Dai, *Electrochem. Energy Rev.* **2018**, *1*, 84.

[107] Y. Liu, R. Wang, Y. Lyu, H. Li, L. Chen, *Energy Environ. Sci.* **2014**, *7*, 677.

[108] S. Xu, S. K. Das, L. A. Archer, *RSC Adv.* **2013**, *3*, 6656.

[109] S. Liu, H. B. Yang, X. Huang, L. H. Liu, W. Z. Cai, J. J. Gao, X. N. Li, T. Zhang, Y. Q. Huang, B. Liu, *Adv. Funct. Mater.* **2018**, *28*, 1800499.

[110] Q. Wang, Y. Lei, D. Wang, Y. Li, *Energy Environ. Sci.* **2019**, *12*, 1730.

[111] P. P. Sharma, J. Wu, R. M. Yadav, M. Liu, C. J. Wright, C. S. Tiwary, B. I. Yakobson, J. Lou, P. M. Ajayan, X. D. Zhou, *Angew. Chem., Int. Ed.* **2015**, *54*, 13701.

[112] V. V. Strelko, V. S. Kuts, P. A. Throwerb, *Carbon* **2000**, *38*, 1499.

[113] H. Wang, K. Xie, Y. You, Q. Hou, K. Zhang, N. Li, W. Yu, K. P. Loh, C. Shen, B. Wei, *Adv. Energy Mater.* **2019**, *9*, 1901806.

[114] Y. Jin, C. Hu, Q. Dai, Y. Xiao, Y. Lin, J. W. Connell, F. Chen, L. Dai, *Adv. Funct. Mater.* **2018**, *28*, 1804630.

[115] L. Qie, Y. Lin, J. W. Connell, J. Xu, L. Dai, *Angew. Chem., Int. Ed.* **2017**, *56*, 6970.

[116] J. Gu, C. S. Hsu, L. Bai, H. M. Chen, X. Hu, *Science* **2019**, *364*, 1091.

[117] C. Zhang, S. Yang, J. Wu, M. Liu, S. Yazdi, M. Ren, J. Sha, J. Zhong, K. Nie, A. S. Jalilov, Z. Li, H. Li, B. I. Yakobson, Q. Wu, E. Ringe, H. Xu, P. M. Ajayan, J. M. Tour, *Adv. Energy Mater.* **2018**, *8*, 1703487.

[118] C.-Y. Su, H. Cheng, W. Li, Z.-Q. Liu, N. Li, Z. Hou, F.-Q. Bai, H.-X. Zhang, T.-Y. Ma, *Adv. Energy Mater.* **2017**, *7*, 1602420.

[119] H. Zhang, J. Li, S. Xi, Y. Du, X. Hai, J. Wang, H. Xu, G. Wu, J. Zhang, J. Lu, J. Wang, *Angew. Chem., Int. Ed.* **2019**, *58*, 14871.

[120] X. Zou, X. Huang, A. Goswami, R. Silva, B. R. Sathe, E. Mikmekova, T. Asefa, *Angew. Chem., Int. Ed.* **2014**, *53*, 4372.

[121] J. Wang, X. Li, B. Cui, Z. Zhang, X. Hu, J. Ding, Y. Deng, X. Han, W. Hu, *Rare Met.* **2021**, *40*, 3019.

[122] H. Fei, J. Dong, Y. Feng, C. S. Allen, C. Wan, B. Volosskiy, M. Li, Z. Zhao, Y. Wang, H. Sun, P. An, W. Chen, Z. Guo, C. Lee, D. Chen, I. Shakir, M. Liu, T. Hu, Y. Li, A. I. Kirkland, X. Duan, Y. Huang, *Nat. Catal.* **2018**, *1*, 63.

[123] X. F. Yang, A. Wang, B. Qiao, J. Li, J. Liu, T. Zhang, *Acc. Chem. Res.* **2013**, *46*, 1740.

[124] F. Polo-Garzon, Z. Bao, X. Zhang, W. Huang, Z. Wu, *ACS Catal.* **2019**, *9*, 5692.

[125] H. Zhao, C. Wang, R. Vellacheri, M. Zhou, Y. Xu, Q. Fu, M. Wu, F. Grote, Y. Lei, *Adv. Mater.* **2014**, *26*, 7654.

[126] B. Burger, P. M. Maffettone, V. V. Gusev, C. M. Aitchison, Y. Bai, X. Wang, X. Li, B. M. Alston, B. Li, R. Clowes, N. Rankin, B. Harris, R. S. Sprick, A. I. Cooper, *Nature* **2020**, *583*, 237.

[127] K. T. Butler, D. W. Davies, H. Cartwright, O. Isayev, A. Walsh, *Nature* **2018**, *559*, 547.

[128] J. R. Kitchin, *Nat. Catal.* **2018**, *1*, 230.

[129] A. Mazheika, Y. G. Wang, R. Valero, F. Vines, F. Illas, L. M. Ghiringhelli, S. V. Levchenko, M. Scheffler, *Nat. Commun.* **2022**, *13*, 419.

[130] Q. Nian, X. Zhang, Y. Feng, S. Liu, T. Sun, S. Zheng, X. Ren, Z. Tao, D. Zhang, J. Chen, *ACS Energy Lett.* **2021**, *6*, 2174.

[131] S. E. Renfrew, D. E. Starr, P. Strasser, *ACS Catal.* **2020**, *10*, 13058.

[132] M. Sha, H. Zhao, Y. Lei, *Adv. Mater.* **2021**, *33*, 2103304.

[133] J. Qiu, H. Zhao, Y. Lei, *SmartMat* **2022**, *3*, 447.

Changfan Xu received his M.S. degree in Metallurgical Engineering from Central South University in 2021. He is currently a Ph.D. Candidate under the supervision of Prof. Yong Lei at the Technical University of Ilmenau in Germany. His research interests focus on the construction and functionalization of nanomaterials for energy storage and conversion.

ADVANCED
SCIENCE NEWS

www.advancedsciencenews.com

NANO · MICRO
small
www.small-journal.com

Yulian Dong received her Master degree in the School of Environmental and Chemical Engineering, Shanghai University in 2019. She is currently being sponsored by China Scholarship Council (CSC) as a Ph.D. Candidate at Technology University of Ilmenau under the supervision of Prof. Yong Lei. Her research interests focus on functional nanostructures for sodium and potassium ion batteries.

Yonglong Shen received his B.Sc. degree and M.Sc. degree in Materials Science from Zhengzhou University in 2006 and in 2009, respectively. He came to UK in 2010, received a Ph.D. degree in Materials Science from University of Bolton in 2015. He then spent 2 years as a Postdoctoral Fellow at Zhengzhou University and has been a lecture since 2018. His research interests include semiconductors, thin films, electrical and optical properties of metal oxides, and advanced characterization techniques (TEM and EELS).

Huaping Zhao obtained his Ph.D. in Materials Science from the State Key Laboratory of Crystal Materials of Shandong University in 2007. Following 2 years of postdoctoral research at the Institute of Chemistry (Chinese Academy of Sciences, 2007–2009), he was employed as a Scientist by the University of Muenster from 2009 to 2011. Since 2012, he has been a Senior Scientist (permanent) in Prof. Yong Lei's group at the Technical University of Ilmenau, Germany. His current research focus is the design and fabrication of functional nanostructures for energy storage and conversion.

Liqiang Li earned his Ph.D. degree in 2008 from Institute of Chemistry, Chinese Academy of Sciences. After that, he worked as Postdoctoral Researcher in Muenster. In 2014 he joined Suzhou Institute of Nano-Tech and Nano-Bionic, Chinese Academy of Sciences as a Principal Investigator. He is now a Professor in Institute of Molecular Aggregation Science, Tianjin University since 2019. His research interests include the materials and devices in organic field-effect transistors, and especially focus on the stability, controlled assembly, doping, and charge transport mechanisms of organic semiconductors.

Guosheng Shao is Professor and the Director of the State Centre for International Cooperation on Designer Low-carbon and Environmental Materials (CDLCEM) at the Zhengzhou University, China. He is also the founding director of the Zhengzhou Materials Genome Institute (ZMGI, 2016-) and Visiting Professor to the University of Surrey, UK (2018-). He earned his Ph.D. in materials science at the University of Surrey and then worked across UK universities as senior academic member. His current focus is on sustainable (renewable) energy systems and environmental materials technologies. He serves as Editor-in-Chief of Energy & Environmental Materials.

Yong Lei is Professor and Head of Group (Chair) of Applied Nano-Physics at the Technical University of Ilmenau, Germany. He began working in Germany in 2003 as an Alexander von Humboldt Fellow at the Karlsruhe Institute of Technology. From 2006, he was a group leader at the University of Muenster and a juniorprofessor. In 2011, he joined the Technical University of Ilmenau as a Chair Professor. His research focuses include template nanostructuring, energy conversion andstorage devices, and optoelectronic applications of nanostructures. He hasreceived a few prestigious European and German funding including two European Research Council Grants.

2206445 (30 of 30)